

1 Long- and short-read metabarcoding technologies reveal  
2 similar spatio-temporal structures in fungal communities

3 Brendan Furneaux<sup>1,\*</sup>, Mohammad Bahram<sup>2,3</sup>, Anna Rosling<sup>4</sup>,  
4 Nourou S. Yorou<sup>5</sup>, Martin Ryberg<sup>1</sup>

5 <sup>1</sup>Program in Systematic Biology, Department of Organismal Biology,  
6 Uppsala University, Uppsala, Sweden

7 <sup>2</sup>Department of Ecology, Swedish University of Agricultural Sciences,  
8 Uppsala, Sweden

9 <sup>3</sup>Institute of Ecology and Earth Sciences, University of Tartu, Tartu, Estonia

10 <sup>4</sup>Program in Evolutionary Biology, Department of Ecology and Genetics,  
11 Uppsala University, Uppsala, Sweden

12 <sup>5</sup>Research Unit in Tropical Mycology and Plant-Fungi Interactions, LEB,  
13 University of Parakou, Parakou, Benin

14 \*Corresponding author, [brendan.furneaux@ebc.uu.se](mailto:brendan.furneaux@ebc.uu.se)

## 15 **Abstract**

16 Fungi form diverse communities and play essential roles in many terrestrial ecosystems, yet  
17 there are methodological challenges in taxonomic and phylogenetic placement of fungi from  
18 environmental sequences. To address such challenges we investigated spatio-temporal struc-  
19 ture of a fungal community using soil metabarcoding with four different sequencing strategies:  
20 short amplicon sequencing of the ITS2 region (300–400 bp) with Illumina MiSeq, Ion Torrent  
21 Ion S5, and PacBio RS II, all from the same PCR library, as well as long amplicon sequenc-  
22 ing of the full ITS and partial LSU regions (1200–1600 bp) with PacBio RS II. Resulting  
23 community structure and diversity depended more on statistical method than sequencing  
24 technology. The use of long-amplicon sequencing enables construction of a phylogenetic tree  
25 from metabarcoding reads, which facilitates taxonomic identification of sequences. However,  
26 long reads present issues for denoising algorithms in diverse communities. We present a  
27 solution that splits the reads into shorter homologous regions prior to denoising, and then  
28 reconstructs the full denoised reads. In the choice between short and long amplicons, we  
29 suggest a hybrid approach using short amplicons for sampling breadth and depth, and long  
30 amplicons to characterize the local species pool for improved identification and phylogenetic  
31 analyses.

## 32 **1 Introduction**

33 Fungi are key drivers of nutrient cycling in terrestrial ecosystems. One important guild of  
34 fungi form ectomycorrhizas (ECM), a symbiosis between fungi and plants in which fungal  
35 hyphae enclose the plant’s fine root tips. The fungi provide nutrients and protection from  
36 pathogens in exchange for carbon from the plant (Smith & Read, 2010). Approximately 8%  
37 of described fungal species are thought to take part in ECM symbiosis (Ainsworth, 2008;

38 Rinaldi et al., 2008). Although only about 2% of land plant species form ECM, these include  
39 ecologically and economically important stand-forming trees belonging to both temperate and  
40 boreal groups such as Pinaceae and Fagaceae, and tropical groups such as Dipterocarpaceae,  
41 *Uapaca* (Phyllanthaceae) and Fabaceae tr. Amherstieae (Brundrett, 2017), together repre-  
42 senting approximately 60% of tree stems globally (Steidinger et al., 2019).

43 Although ECM fungi form many well-known mushrooms (e.g., *Amanita*, *Cantharellus*, *Bole-*  
44 *tus*), some instead produce inconspicuous (e.g., *Tomentella*) or no (e.g., *Cenococcum*) fruit  
45 bodies. Even when fruitbodies are large, they are ephemeral, so study of ECM communities  
46 is facilitated by sampling of vegetative structures (Horton & Bruns, 2001). Unlike many  
47 saprotrophic fungi which grow easily in axenic culture, ECM fungi are usually difficult to  
48 culture, so DNA barcoding is increasingly used to investigate vegetative structures in the  
49 field. The advent of high-throughput sequencing (HTS) has facilitated such studies by pro-  
50 viding enough sequencing depth for metabarcoding of bulk environmental samples such as  
51 soils (Lindahl et al., 2013).

52 As additional techniques and methods are developed for HTS, there is an increasing array  
53 of choices for researchers investigating fungal communities. Fungal metabarcoding studies  
54 using short-read HTS technologies such as 454 Pyrosequencing, Illumina, and Ion Torrent  
55 have usually targeted the rDNA internal transcribed spacer regions ITS1 or ITS2, which  
56 are the standard molecular barcode for fungi, providing sufficient resolution to distinguish  
57 fungal species in many groups, and which are usually short enough for HTS (Lindahl et al.,  
58 2013; Schoch et al., 2012). In some groups such as arbuscular mycorrhizal fungi, variable  
59 regions of the rDNA small subunit (SSU) are the barcode of choice (Öpik et al., 2010), and  
60 variable regions of the rDNA large subunit (LSU) have also been used for barcoding (House  
61 et al., 2016; Tedersoo et al., 2015). The resulting sequencing reads are clustered by sequence  
62 similarity to form operational taxonomic units (OTUs), which are then used as the units for  
63 further community analysis (Lindahl et al., 2013). If taxonomic identification is desired in

64 order to put OTUs in a wider context and associate functional information, it has usually  
65 been performed by database searches using BLAST (Altschul et al., 1990; Lindahl et al.,  
66 2013) with public databases such as GenBank (Benson et al., 2013) and Unite (Nilsson et al.,  
67 2019). However, this approach comes with some potential weaknesses, discussed below.

68 Different sequencing technologies have different capabilities in terms of sequencing depth and  
69 read length, as well as differing quality profiles and potential biases (Yang et al., 2013). The  
70 rapid development of new HTS technologies, as well as subsequent iterative improvements in  
71 sequencing chemistry and read capacity, means that the technologies used in metabarcoding  
72 studies, along with any associated biases, change frequently. As an example, the first study  
73 using HTS metabarcoding of soil fungi was published in 2009 (Buée et al., 2009) using 454  
74 Pyrosequencing; production of 454 sequencers was subsequently discontinued in 2015, and  
75 sales of reagents stopped in 2016 (Hollmer, 2013). This brings into question the comparability  
76 of studies conducted only a few years apart.

77 ITS1 and ITS2 often have suitable variation to distinguish species, although closely related  
78 species may share identical ITS sequences in certain groups such as various Pezizomycotina  
79 (Schoch et al., 2012), but this variability means that they cannot be reliably aligned over the  
80 fungal kingdom (Lindahl et al., 2013; Tedersoo, Tooming-Klunderud, et al., 2018). Addi-  
81 tionally, the wide range of length variation of these regions may introduce bias in recovery of  
82 different taxa (Ihrmark et al., 2012; Palmer et al., 2018; Tedersoo et al., 2015). Further bias  
83 is introduced by variation in the 5.8S region which separates the two ITS regions, as well as  
84 in the 5' end of LSU, which makes it difficult to design primers that are suitable for all fungi  
85 (Tedersoo et al., 2015).

86 Distance-based clustering conflates intra-species variation and sequencing error, and results  
87 are dataset-specific. In contrast, more recent denoising methods such as DADA2 (Callahan  
88 et al., 2017), Deblur (Amir et al., 2017), and UNOISE2 (Edgar, 2016b) utilize read quality

89 information to control for sequencing error while preserving intra-species variation. The  
90 resulting units are known as amplicon sequence variants (ASVs) or exact sequence variants  
91 (ESVs), as they should represent true amplicon sequences from the sample. Unlike cluster-  
92 based OTUs, ASVs can capture variation of as little as one base pair, although alpha and  
93 beta diversity estimates based on ASVs and OTUs at different clustering thresholds are highly  
94 correlated (Botnen et al., 2018; Glassman & Martiny, 2018). ASVs have been suggested to be  
95 less dataset specific than cluster-based OTUs (Callahan et al., 2017). Support for PacBio has  
96 recently been added to DADA2 (Callahan et al., 2019), but its application requires greater  
97 sequencing depth for longer reads, especially in high diversity samples.

98 Because both OTU clustering and denoised ASVs may “clump” different species into a single  
99 unit and “split” a single species into multiple units (Ryberg, 2015), diversity measures based  
100 on counting species within a community or shared species between two communities may give  
101 different results depending on the clustering threshold. In contrast, phylogenetic community  
102 distance measures (Wong et al., 2016) are relatively insensitive to species/OTU delimitation,  
103 but require a phylogenetic tree. Phylogenetic placement algorithms have been developed to  
104 place short amplicon reads onto a reference tree (Berger et al., 2011; Matsen et al., 2010),  
105 but are not easy to apply to ITS sequences because they require that the query sequences be  
106 aligned to a reference alignment. Additionally, methods exist to place OTUs on a simplified  
107 tree based on taxonomic assignments (Tedersoo, Sánchez-Ramírez, et al., 2018), or to create  
108 hybrid trees using ITS and a more conserved marker such as SSU or LSU based on matching  
109 taxonomic annotations in reference databases (Fouquier et al., 2016), but these approaches  
110 are only applicable to sequences of known taxonomic affiliation.

111 Assignment of taxonomic identities to environmental sequences is dependent on both the  
112 reference database and the algorithm used. Although the public INSDC databases (Karsch-  
113 Mizrachi et al., 2018) are often used for sequence identification, the open nature of submission  
114 to these databases results in a substantial fraction of incorrect taxonomic annotations (Nilsson

115 et al., 2006; Steinegger & Salzberg, 2020) as well as sequences of poor technical quality  
116 (Nilsson et al., 2012). Consequently taxonomic assignments based on these databases may  
117 be incorrect or inconsistent. Several curated databases also exist which attempt to address  
118 these issues and which cover the whole fungal kingdom. The Unite database is a more curated  
119 attempt to include all publically available ITS sequences (800 000 as of release 8.0), originally  
120 targetting fungi but now expanded to include all eukaryotes (Nilsson et al., 2019), where  
121 efforts have been made to correct incorrect annotations and exclude low-quality sequences  
122 (Abarenkov et al., 2018). The Ribosomal Data Project (RDP, Cole et al., 2014) hosts two  
123 manually curated fungal barcode sequence databases, which are specifically intended for use  
124 in taxonomic assignment of sequences: the Warcup ITS database, containing 18 000 manually  
125 curated fungal ITS sequences (Deshpande et al., 2016), and the RDP fungal LSU training set,  
126 containing 8000 manually curated LSU sequences from fungi and 3000 from other eukaryotic  
127 groups (Liu et al., 2012). Although the quality of sequences and taxonomic annotations is  
128 undoubtedly higher in these more curated databases, they are inherently limited in taxonomic  
129 coverage and do not include the most recently published sequences.

130 Assigning taxonomy to unknown sequences using BLAST requires *a priori* choice of simi-  
131 larity thresholds for different taxonomic ranks. Several algorithms specifically designed for  
132 taxonomic assignment have been published which instead use information about variability  
133 within different taxa in the reference database to assign unknown sequences, along with con-  
134 fidence estimates for these assignments, including the RDP Classifier (RDPC, Wang et al.,  
135 2007), SINTAX (Edgar, 2016a) and IDTAXA (Murali et al., 2018) among others. In addi-  
136 tion, methods have been published which integrate predictions from multiple algorithms to  
137 increase the reliability of assignments (Gdanetz et al., 2017; Palmer et al., 2018; Somervuo  
138 et al., 2016). However, all sequence-similarity based approaches are dependent on high tax-  
139 onomic coverage in the reference database, making the placement of novel or undersampled  
140 groups problematic (Nilsson et al., 2016; Tedersoo, Tooming-Klunderud, et al., 2018).

141 Recent long-read HTS technologies such as Pacific Biosciences (PacBio) Single Molecule Real  
142 Time (SMRT) sequencing enable sequencing longer amplicons which include both the ITS  
143 regions and the flanking, more highly conserved SSU and/or LSU regions. This can improve  
144 taxonomic placement of sequences that lack close database matches and allow the alignment  
145 of metabarcoding reads for subsequent phylogenetic analysis (Tedersoo, Tooming-Klunderud,  
146 et al., 2018). Information from phylogenetic trees produced from long-amplicon metabarcod-  
147 ing has the potential to both improve taxonomic assignment and provide alternative measures  
148 of community alpha and beta diversity. However, long-read technologies are currently more  
149 expensive per read compared to short-read sequencing, and so their use entails a trade-off  
150 with sequencing depth and/or sample number (Kennedy et al., 2018).

151 Because of the variety of sequencing platforms and analytical pipelines which have been used  
152 in metabarcoding studies, comparisons between studies may be difficult. Here we investigated  
153 the effects of different sequencing strategies and post-analysis on biological conclusions using  
154 measurement of the spatiotemporal turnover rate of the fungal community in an ECM-  
155 dominated woodland in Benin by metabarcoding of bulk soil, sampled at narrow intervals,  
156 over two years. Turnover scale is the distance at which two communities can be considered to  
157 be independent samples of the local species pool. Knowledge of turnover scale is important  
158 when planning studies of local diversity and its environmental correlates. Turnover scale  
159 varies between different ecosystems and taxonomic groups, and can be measured by the range  
160 at which a Mantel correlogram indicates significant autocorrelation, or by fitting a function  
161 to an empirical distance-decay curve of community dissimilarity vs. distance (Legendre &  
162 Legendre, 2012).

163 We compare three different sequencing platforms (PacBio RS II, Illumina MiSeq, Ion Tor-  
164 rent Ion S5), long and short amplicons, three different taxonomic assignment algorithms  
165 (RDP classifier, SINTAX, IDTAXA) with three different reference databases (Unite, War-  
166 cup, RDP), and both non-phylogenetic and phylogenetic community distance measures. We

167 also present new algorithms for dividing the LSU into domains, combining denoising results  
168 from multiple domains as a strategy to capture more ASVs from long amplicons in diverse  
169 communities, and incorporating phylogenetic information into taxonomic assignments.

## 170 **2 Materials and Methods**

### 171 **2.1 Sampling**

172 Sampling was conducted at two sites, near the villages of Angaradebou (Ang: N 9.75456°  
173 E 2.14064°) and Gando (Gan: N 9.75678° E 2.31058°) approximately 30 km apart in the  
174 *Forêt Classée de l'Ouémé Supérieur* (Upper Ouémé Forest Reserve) in central Benin. Both  
175 sites were located in West Sudanian savannah woodlands (Olson et al., 2001; Yorou et al.,  
176 2014) dominated by the ECM host tree *Isoberlinia doka* (Caesalpinioideae). At each site,  
177 25 soil samples were collected along a single 24 m linear transect at intervals of 1 m in May  
178 2015. One third of the sample locations (3 m spacing) were resampled one year later in June  
179 2016, for a total of 67 samples. For each sample, coarse organic debris was removed from  
180 the soil surface and a sample of approximately 5 cm × 5 cm × 5 cm was extracted with a  
181 sterilized knife blade and homogenized. A subsample of approximately 250 mg was preserved  
182 and returned to the laboratory for extraction (see Supplementary methods).

### 183 **2.2 DNA amplification and sequencing**

184 DNA extracts were sequenced using four distinct strategies, with two different amplicon  
185 lengths (long and short; Figure 1a) and three different technologies (PacBio, Ion Torrent,  
186 and Illumina) for the short amplicon. Due to length limitations of Ion Torrent and Illumina  
187 sequencing, long amplicons were only sequenced with PacBio. The short amplicon (approxi-

188 mately 300 bp) targeted the full ITS2 region as well as parts of the flanking 5.8S and large  
189 subunit (LSU) rDNA, using gITS7 (Ihrmark et al., 2012) as the forward primer and a mix  
190 of ITS4 (White et al., 1990) and ITS4a (Urbina et al., 2016) as the reverse primer. The long  
191 amplicon (approximately 1500 bp) targeted the full ITS region including the 5.8S rDNA and  
192 approximately 950 bp at the 5' end of the LSU, including the first three variable regions  
193 (Figure 1a), using ITS1 (White et al., 1990) as the forward primer and LR5 (Vilgalys &  
194 Hester, 1990) as the reverse primer. Each PCR run also included a blank sample and a posi-  
195 tive control consisting of freshly extracted DNA from a commercially purchased fruitbody of  
196 *Agaricus bisporus*. See Supplementary methods for PCR and library preparation protocols.

197 Each library was sequenced on a PacBio RS II sequencer at the Uppsala Genome Center  
198 (UGC; Uppsala Genome Center, Science for Life Laboratory, Dept. of Immunology, Ge-  
199 netics and Pathology, Uppsala University, BMC, Box 815, SE-752 37 UPPSALA, Sweden).

200 Short amplicon libraries were sequenced on two SMRT cells each, while long amplicon li-  
201 braries were sequenced on four SMRT cells each. Additionally, the same short amplicon  
202 PCR libraries were combined and sequenced using an Ion S5 (Ion Torrent) sequencer using  
203 one 520 chip at UGC, and a MiSeq (Illumina Inc.) sequencer using v3 chemistry with a  
204 paired-end read length of 300 bp at the SNP&SEQ Technology Platform (Dept. of Medical  
205 Sciences, Uppsala University, BMC, Box 1432, SE-751 44 UPPSALA, Sweden) using one half  
206 of a lane. Platform-specific library preparation, including adapter ligation, was performed at  
207 the sequencing facilities according to their standard protocols.

## 208 **2.3 Bioinformatics**

209 Circular consensus sequence (CCS) basecalls for PacBio sequences were made using `ccs`  
210 version 3.4 (Pacific Biosciences, 2016, July 13/2019) using the default settings. The resulting  
211 sequences, as well as the paired-end Illumina sequences, were demultiplexed and sequencing

212 primers were removed using `cutadapt` version 2.8 (Martin, 2011). Sequencing primers were  
213 similarly removed from the Ion Torrent sequences, but interference between the tagged gITS7  
214 primers and the Ion XPress tags used in library prep made full demultiplexing of the Ion  
215 Torrent sequences impossible, resulting in two samples sharing each tag. These reads were  
216 thus either analyzed as a pool, or comparisons were made to equivalently combined samples  
217 in the other datasets. For Ion Torrent and PacBio, reads were discarded if they did not have  
218 the appropriate primers on both ends. Reads were searched in both directions, and reads  
219 where the primers were found in the reverse direction were reverse complemented before  
220 further analysis. For Illumina sequences, read pairs were only retained when PCR primers  
221 were detected at the 5' ends of both the forward and reverse read. Primers were also searched  
222 for and removed on the 3' ends of the reads, in case of readthrough with short amplicons.  
223 Read pairs where the primers were found in reverse orientation were kept in separate files,  
224 but were retained in their original orientation until after denoising.

### 225 **2.3.1 Denoising and clustering**

226 All amplicons were denoised using DADA2 version 1.12.1 according to the ITS pipeline  
227 workflow (Callahan, 2020a; Callahan et al., 2016), with technology-specific modifications  
228 for Ion Torrent (Callahan, 2020b) and PacBio (Callahan et al., 2019). Although this was  
229 successful for the short amplicons on all technologies, only 38 ASVs were obtained for the  
230 long amplicons, representing 12% of the trimmed reads.

231 We conclude that this poor performance was due to a combination of long amplicon length  
232 and low sequencing depth relative to community diversity (see Supplementary Methods). We  
233 therefore developed a new workflow to assemble ASVs from the long amplicons by splitting  
234 the reads into homologous domains, including the two ITS regions, 5.8S, the variable D1–3  
235 regions of LSU (Michot et al., 1984), and the conserved LSU regions between the D regions,

236 here referred to as LSU1–4 (Figure 1a), followed by independently denoising reads from  
237 each domain, concatenating the denoised domains, and finally forming consensus sequences  
238 based on ITS2 identity. We used this method, implemented in the new R packages `LSUx`  
239 (<https://github.com/brendanf/LSUx>) and `tzara` (<https://github.com/brendanf/tzara>) and  
240 detailed in the Supplementary Methods, for all of the PacBio and Ion Torrent datasets.

241 Because the `LSUx` plus `tzara` method as currently implemented is not applicable to Illumina  
242 paired-end reads, the ASVs generated from the Illumina dataset according to the standard  
243 DADA2 workflow were used. The ITS2 region was extracted from the ASVs using `LSUx` for  
244 comparison to the results from the other technologies.

245 To account for intra-species variation and the possibility of different denoising performance  
246 between the different sequencing strategies, the pooled ITS2-ASVs from all sequencing strate-  
247 gies were also clustered into operational taxonomic units (OTUs) at 97% similarity using  
248 VSEARCH v2.9.1 (Rognes et al., 2016).

### 249 **2.3.2 Phylogenetic inference and taxonomy assignment**

250 Full length long amplicon ASVs were aligned using DECIPHER (Wright, 2015) with up to  
251 10 iterations of alternating progressive alignment and conserved RNA secondary structure  
252 calculation, followed by 10 refinement iterations. This alignment was truncated at a position  
253 after the D3 region corresponding to base 907 of the *Saccharomyces cerevisiae* S288C reference  
254 sequence for LSU, because several sequences had introns after this position, as also observed in  
255 several fungal species by Holst-Jensen et al. (1999). An ML tree was produced using RAxML  
256 version 8.2.12 (Stamatakis, 2014) using the GTR+GAMMA model and rapid bootstrapping  
257 with the MRE\_IGN stopping criterion. The tree was rooted outside kingdom Fungi and  
258 non-Fungi were removed based on taxonomic assignments (see below and Supplementary  
259 methods).

260 Taxonomic annotations of the RDP LSU fungal training set version 11.5 (Cole et al., 2014)  
261 and Warcup ITS training set (Deshpande et al., 2016) were mapped to a uniform taxonomic  
262 classification system (see Supplementary Methods). Preliminary taxonomic assignment was  
263 performed to genus level separately on the ITS region using Unite and Warcup and on the  
264 LSU region using RDP, respectively, as taxonomic references. For each region/reference com-  
265 bination, taxonomy was assigned using three popular algorithms: the RDP Naïve Bayesian  
266 Classifier (RDPC, Wang et al., 2007) as implemented in DADA2; SINTAX (Edgar, 2016a) as  
267 implemented in VSEARCH v2.9.1 (Rognes et al., 2016); and IDTAXA (Murali et al., 2018).  
268 A relatively lax confidence threshold of 50% was used for all three algorithms. Each full-  
269 length ASV was thus given up to nine preliminary taxonomic assignments (three references  
270  $\times$  three algorithms). ASVs from the short-amplicon datasets for which no matching long-  
271 amplicon ASV could be reconstructed were taxonomically assigned using Unite and Warcup  
272 on the full length of the short amplicon.

273 For full-length long-amplicon ASVs, the preliminary taxonomic assignments were refined  
274 using the phylogenetic tree (Figure S4 and Supplementary Methods). This refinement  
275 algorithm is referred to as “PHYLOTAX”, available in the new R package `phylotax` at  
276 <https://github.com/brendanf/phylotax>.

277 ASVs which were not present in the tree, either because they were not represented in the  
278 long-amplicon dataset, or because full-length ASV reconstruction failed, were given refined  
279 taxonomic assignments using a strict consensus of the different preliminary assignments at  
280 each rank, resulting in a consensus assignment equivalent to the “last common ancestor” of the  
281 preliminary assignments. This algorithm has been used to assign a consensus taxonomy based  
282 on a list of top BLAST hits (LCAClassifier, Lanzén et al., 2012) or k-mer similarity scores  
283 (mothur’s k-nearest neighbor method, Schloss et al., 2009), but here is used to resolve conflicts  
284 between assignments from different algorithms and databases. Strict consensus assignments  
285 were also generated for all ASVs, as a comparison to the PHYLOTAX assignments, and are

286 referred to as “Consensus”.

## 287 **2.4 Effect of sequencing strategy on recovered community**

288 We compared alpha diversity estimates by the different sequencing strategies by calculating  
289 ASV and OTU accumulation curves, as well as comparing richness estimates after rarefac-  
290 tion for each sample (Supplementary methods). We also compared the effect of sequencing  
291 technology and amplicon length on the recovered fungal community composition, as assessed  
292 by the Bray-Curtis dissimilarity, using PERMANOVA and heat tree visualizations (Supple-  
293 mentary methods).

## 294 **2.5 Spatiotemporal analysis**

295 To estimate turnover scale, ecological community dissimilarity matrices were calculated using  
296 the ASV/OTU based Bray-Curtis metric (Bray & Curtis, 1957, for both long and short  
297 amplicons) and the phylogenetically based weighted UniFrac metric (C. Lozupone & Knight,  
298 2005; C. A. Lozupone et al., 2007, for only long amplicons) in `phyloseq` version 1.26.0.  
299 Each of these distance matrices was used to calculate a Mantel correlogram with a 1 m  
300 bin size for distances in the range of 0–12 m, i.e., half the maximum separation present  
301 in the dataset. Separate correlograms were drawn for samples taken during the same year  
302 and samples separated in time by one year, in order to assess the degree to which the soil  
303 community changes over the course of one year.

304 Additionally, empirical spatiotemporal distance-decay curves were generated by plotting  
305 mean community dissimilarity as a function of spatial distance and time lag, and fit to  
306 an exponential model of the form given by Legendre and Legendre (2012) using the `nls`  
307 function in R (Supplementary methods).

### 3 Results

Samples from Ang in 2015 yielded low quantities of DNA, poor PCR performance, and ultimately very few sequencing reads, especially in the long amplicon library, where only one sample produced more than 100 reads (Figure S5). Consequently, Ang samples were excluded from spatial analysis, although they were retained for denoising, phylogenetic reconstruction, and taxonomic assignment.

The number of sequencing reads and ASVs at each stage in the bioinformatics pipeline differed between sequencing strategies (Table S2). Sequencing with PacBio yielded more than twice as many raw reads for long amplicons as for short amplicons, with approximately 125 thousand and 50 thousand reads, respectively. Ion Torrent and Illumina yielded substantially more reads, with 20.7 million and 10.8 million, respectively. PacBio sequencing of the short amplicon library yielded the highest fraction of high-quality reads ( $\leq 1$  expected error), followed by Illumina, with Ion Torrent yielding the lowest quality (Figure S6b). Although the per-base read quality of the long amplicon PacBio sequences was similar to that of Illumina (Figure S6a), this translated to a greater number of expected errors per read due to the amplicon length (Figure S6b). Demultiplexing, primer trimming, and quality filtering reduced the read totals by 64% for PacBio long amplicons, but only by 21% for PacBio short amplicons, resulting in a similar number of filtered reads for the two strategies. Losses in demultiplexing, trimming, and quality filtering were intermediate for Ion Torrent and Illumina, with 41% and 28% loss, respectively. Extraction of only the ITS2 region before quality filtering (Figure S6c) reduced the loss of long amplicon PacBio reads to only 29%, comparable to Illumina. Application of `tzara` resulted in 708 reconstructed long-amplicon ASVs, representing 97% of denoised ITS2 reads from the long-amplicon PacBio dataset. Mapping identical ITS2 ASVs from the short and long amplicon datasets allowed 58%, 71%, and 81% of denoised reads from the Ion Torrent, Illumina, and PacBio short amplicon datasets, respectively, to be assigned

333 to a long amplicon ASV (Table S2).

334 Almost all of the short amplicon sequences from all three technologies were between 240 and  
335 375 bp long (Figure S7a). Although the length profile of the three sequencing runs were  
336 similar, Illumina had the largest fraction of reads near the top of the range, followed by  
337 Ion Torrent and PacBio (Figure S7b). The difference in length distributions was statistically  
338 significant due to the large sample size (Kruskal-Wallis statistic =  $8.57e+04$ ,  $p < 2.2 \times 10^{-16}$ ),  
339 but the difference between means was fairly small, with mean amplicon lengths of 276, 281,  
340 and 286 bp for PacBio, Ion Torrent, and Illumina, respectively. The length of the long  
341 amplicon reads varied widely, from 696 to 1638 bp, with a mean of 1431 bp (Figure S7c).

342 Among the different regions extracted from the long amplicon (Figure S8, ITS1 showed the  
343 greatest length variability (mean  $\pm$  standard deviation:  $193 \pm 55$  bp), followed by ITS2 ( $184$   
344  $\pm 41$  bp) and the variable regions in LSU (D2:  $227 \pm 36$  bp; D3:  $108 \pm 10$  bp; D1:  $159 \pm$   
345  $6$  bp). Approximately 2% of reads included an intron of 40–60 bp in the LSU4 region, not  
346 visible in Figure S8 due to rarity. Except for these sequences, all conserved regions of LSU, as  
347 well as 5.8S, displayed very little size variation, as expected, with standard deviations  $< 2$  bp.  
348 Around 12% of ITS2 sequences extracted from the long amplicon dataset were shorter than  
349 140 bp, a much greater fraction than the 0.26% to 0.44% from the short amplicon datasets  
350 (Figure S9). The taxonomic identity of these sequences is discussed below.

351 *Agaricus bisporus*, the positive control, was represented by a single ASV in the positive control  
352 samples for both long- and short-amplicon PacBio datasets, and in the Ion Torrent dataset.  
353 *A. bisporus* was represented by two ASVs in the Illumina dataset, which differed at one base  
354 pair (99.5% similarity in ITS2). The abundance of the second ASV was 1.1% and 1.0% that  
355 of the primary *A. bisporus* ASV in the two Illumina positive controls. The consistency of this  
356 ratio across replicate positive controls suggests that it represents true inter-copy variation  
357 within the specimen, rather than sequencing or PCR error. Despite higher total sequencing

358 depth, this ASV was not identified from the Ion Torrent dataset.

359 *A. bisporus* sequences represented 0.01%, 0.09%, 0.09%, and 0.09% of non-control reads, in  
360 the PacBio long, PacBio short, Illumina, and Ion Torrent datasets, respectively, giving similar  
361 estimates for the rate of tag-switching for all technologies. These reads were excluded from  
362 community analyses.

### 363 **3.1 Reproducibility of sequence capture using different technolo-** 364 **gies**

365 We compared the unique ASVs and OTUs shared between datasets from different sequencing  
366 strategies, and the number of reads represented by these ASVs and OTUs in each strategy.  
367 The majority of abundant ASVs and OTUs were captured by all sequencing strategies used  
368 (Tables S3 and S4). The short amplicon ASVs shared between all sequencing technologies  
369 represented 95%, 76%, and 66% of the reads for PacBio, Illumina, and Ion Torrent, respec-  
370 tively (Figure 2a). When differences at the intra-species scale were removed by clustering the  
371 ASVs into 97% OTUs, the number of OTUs shared between all three technologies increased  
372 to 524, representing 100%, 93% , and 89% % of reads, respectively (Figure 2b). In particu-  
373 lar, the majority of the 9418 unique Ion Torrent ASVs were found to be shared with other  
374 sequencing technologies upon OTU clustering. ASVs unique to the Ion Torrent dataset made  
375 up 14% of reads in that dataset, but only 1% belonged to a unique OTU after clustering. In  
376 contrast, 21% of reads in the long PacBio dataset belonged to ASVs whose ITS2 region was  
377 unique to that dataset (Figure 2c), and the fraction only reduced to 20% after clustering the  
378 ITS2 regions into OTUs (Figure 2d).

379 Read counts for shared ASVs and OTUs were highly correlated between strategies, with a  
380 minimum  $R^2$  value of 0.47 (Figure S10). Correlations between read counts for the three  
381 technologies using the short amplicon library were increased by OTU clustering (0.69 to

382 0.72, 0.49 to 0.74, and 0.74 to 0.82, for PacBio vs. Illumina, PacBio vs. Ion Torrent, and  
383 Illumina vs. Ion Torrent, respectively), but not between the long amplicon library and short  
384 amplicon library (0.65 to 0.62, 0.58 to 0.57, and 0.47 to 0.49, for PacBio long amplicon reads  
385 vs. PacBio, Illumina, and Ion Torrent short amplicon reads, respectively; Figure S10).

386 ASV richness estimates after rarefaction were strongly correlated between the three sequenc-  
387 ing technologies applied to the short amplicon library ( $R^2 = 0.91$  to  $0.94$ ; Figure 4). The  
388 slope of the relationship between PacBio and Illumina richness estimates was only slightly  
389 different from 1, indicating that these two technologies give highly comparable rarefied rich-  
390 ness estimates, despite the approximately  $200\times$  difference in original sequencing depth. Ion  
391 Torrent resulted in rarefied richness estimates which were 24% to 31% greater than the other  
392 technologies, an effect which is also visible in ASV accumulation curves (Figure 3). ASV  
393 richness estimates were somewhat less strongly correlated between the PacBio long amplicon  
394 dataset and the three short amplicon datasets ( $R^2 = 0.65$  to  $0.72$ ; Figure 4). Total least  
395 squares regression indicated that the long amplicon dataset resulted in richness estimates  
396 which were intermediate between the short amplicon results from Ion Torrent and the other  
397 two technologies. Despite the fact that experiment-wide OTU richness was lower than ASV  
398 richness (Figure 2), sample-wise OTU accumulation curves (Figure S11) and rarefied OTU  
399 richness relationships between sequencing strategies (Figure S12) were highly similar to those  
400 for ASVs.

## 401 **3.2 Taxonomic assignment**

402 For all sequencing datasets and taxonomic assignment protocols, a higher proportion of  
403 reads were assigned than of ASVs, indicating that common ASVs were more likely to be  
404 taxonomically identified than rare ASVs (Figure 5). A greater fraction of ITS reads and  
405 ASVs were assigned using the Unite database than the Warcup database across sequencing

406 technologies, amplicons, algorithms, and taxonomic ranks. At most taxonomic ranks, the  
407 RDPC algorithm assigned the greatest fraction of reads and ASVs, followed by SINTAX,  
408 and then IDTAXA.

409 Taxonomic composition of the sequenced soil fungal community at the class level is summa-  
410 rized in Figure 6 and as a heat tree (Foster et al., 2017) in Figure S13. The ML tree for  
411 fungal ASVs, along with taxonomic assignments, is shown in Supplementary File 3. Accord-  
412 ing to the PHYLOTAX assignments, Fungi represented 88% of the ASVs and 81% of the  
413 reads in the long amplicon library, compared to 92.4%–96.5% of the ASVs and 97.9%–98.5%  
414 of the reads in the short amplicon library. Many of the ASVs which were unique to the  
415 long-amplicon library thus fall outside kingdom Fungi (Figure S14). In particular a large  
416 fraction of ITS2 sequences with length less than 140 (Figure S9) were identified as Alveolates  
417 (Figure S15).

418 Measured fungal community composition at the class level varied significantly between long  
419 and short amplicons (PERMANOVA with 9999 permutations,  $p < 0.0001$ ,  $R^2 = 0.046$ ), but  
420 only marginally between sequencing technologies ( $p = 0.0669$ ,  $R^2 = 0.002$ ). The majority of  
421 variation was spatiotemporal (i.e., between samples;  $p < 0.0001$ ,  $R^2 = 0.90$ ), but once this  
422 variation was removed, the remaining effect consisted of a clear bias against Sordariomycetes  
423 in the long amplicon dataset (Figures 6, S14, and S18). Additionally, several lower-rank  
424 taxonomic groups showed increased detection in either the long or short datasets, such as  
425 Tulasnellaceae (Agaricomycetes) and Pyronemataceae (Pezizomycetes) in the long amplicon  
426 dataset, and *Myerozyma* (Saccharomycetes) in the short amplicon datasets (Figures S14 and  
427 S17).

428 Fungi categorized as ECM made up 8.9% of ASVs and 39.2% of reads in the long amplicon  
429 library, and 5.4%–13.4% of the ASVs and 36.4%–46.4% of the reads in the short amplicon  
430 library (Figure S16). Although amplicon length had a significant effect on ECM community

431 composition at the family level (Figure S17), the explained variation was very low (PER-  
432 MANOVA with 9999 permutations,  $p = 0.0040$ ,  $R^2 = 0.002$ ), and the majority of variation  
433 was again spatiotemporal ( $p < 0.0001$ ,  $R^2 = 0.98$ ). Variation between sequencing technolo-  
434 gies was not significant ( $p = 0.76$ ,  $R^2 = 0.0002$ ).

### 435 **3.3 Spatial analysis**

436 Results of spatial analysis based on the Bray-Curtis dissimilarity were qualitatively similar  
437 between the two amplicon libraries and between PacBio and Illumina sequencing, with sig-  
438 nificant autocorrelation at  $p < 0.05$  for ranges of up to 2–3 m for the total fungal community,  
439 and 1–2 m for the ECM fungal community (Figure S19). In both cases, the greatest corre-  
440 lation magnitudes were found with Illumina, followed by long amplicon PacBio. The least  
441 spatial structure was detected with PacBio short amplicon sequencing.

442 The Bray-Curtis metric showed positive correlation when resampling at the same locations  
443 one year later (i.e., spatial distance of 0 m, time lag of 1 year), for both the total fungal and  
444 ECM fungal communities, although this result did not reach statistical significance for all  
445 sequencing strategies. This spatiotemporal correlation did not extend to a range of 1 m, and  
446 in fact correlation was negative at a time lag of 1 year and distance of 1 m, indicating that  
447 samples collected 1 m apart in different years were more different than randomly selected  
448 pairs of samples. This negative correlation, which reached marginal statistical significance in  
449 the PacBio short amplicon dataset, was probably a statistical artifact.

450 In contrast to the Bray-Curtis distance, the weighted UniFrac distance showed very little  
451 spatial structure, with only the total fungal community in the 1 m distance class showing  
452 a significant correlation at  $p < 0.05$ . No temporal correlation was found for the weighted  
453 UniFrac distance.

454 The best fit spatial turnover ranges based on Bray-Curtis distance-decay curves calculated

455 from different sequencing strategies range widely from 13–31 m for the total fungal community  
456 and 12–42 m for the ECM fungal community (Figure 7, Table S5). However, there was overlap  
457 of the 95% confidence intervals for all of the Bray-Curtis spatial ranges in both the total fungal  
458 and ECM fungal communities, across amplicon libraries and sequencing technologies, so no  
459 strong conclusion of variability between methods can be drawn. Although a distance-decay  
460 model was fit for the weighted UniFrac distance applied to the total fungal community, the  
461 result was very poorly constrained, and a range of 0 m, indicating no spatial structure, was  
462 included in the 95% confidence interval.

## 463 **4 Discussion**

### 464 **4.1 Reconstruction of long amplicons from denoised subregions**

465 Sequencing depth in the long amplicon PacBio dataset was not sufficient to successfully  
466 denoise using standard protocols, given the amplicon length and diversity of the samples.  
467 ASV recovery for long amplicons using DADA2 was dramatically improved from 12% to  
468 76% of reads by denoising homologous subregions independently using our new `LSUx` and  
469 `tzara` packages. Although newer sequencing platforms from PacBio (Sequel and Sequel II)  
470 feature increased sequencing depth and lower error rate compared to the RS II, long se-  
471 quences inherently require much more sampling depth to identify ASVs. Thus, `tzara` should  
472 increase recovery of rare ASVs from these platforms as well. It may also be adaptable to  
473 Oxford Nanopore sequencing, which has hitherto posed difficulties for application to complex  
474 community metabarcoding (Loit et al., 2019).

## 475 4.2 Comparison of sequencing strategies

476 The three sequencing technologies gave similar results for the short amplicon library, the  
477 major difference being in sequencing depth. Although a greater fraction of PacBio raw  
478 reads were ultimately mapped to ASVs (75%) compared to Illumina (63%) or Ion Torrent  
479 (65%), the latter two technologies provided much greater sequencing depth for a similar cost,  
480 allowing a greater diversity of rare ASVs to be recovered, and were much closer to saturation  
481 of their respective species accumulation curves (Figure 3). OTU read counts were strongly  
482 correlated between technologies ( $R^2 = 0.72\text{--}0.82$ ), and even between primer pairs ( $R^2 = 0.49\text{--}$   
483  $0.62$ , Figure S10b), which we interpret as supporting the validity of abundance-based beta  
484 diversity measures in metabarcoding (but see Castaño et al., 2020, and references therein).

485 DADA2 denoising may perform differently on different technologies (or perhaps sequencing  
486 runs), indicated by the fact that clustering ASVs at 97% led to substantially higher cor-  
487 respondence between both the set of OTUs recovered from the same library by different  
488 technologies and the read counts for each OTU (Figure S10). ASV diversity appears to be  
489 artificially inflated in the Ion Torrent dataset relative to the Illumina and PacBio datasets,  
490 which gave remarkably similar ASV richness after rarefaction, despite a difference of around  
491 200x in unrarefied sequencing depth (Figures 2 and 4). This may be a result of the lower  
492 fraction of very high quality reads in the Ion Torrent dataset (Figure S6). We used options for  
493 DADA2 intended to improve performance on technologies, like Ion Torrent, with higher rates  
494 of homopolymer indel errors (Callahan, 2020b), but our results suggest that this still does  
495 not result in performance comparable to that which DADA2 achieves on Illumina sequences,  
496 for which it was developed (Callahan et al., 2016).

497 Although the longer read length capabilities of PacBio allow recovery of longer ITS2 sequences  
498 than the other two technologies, as has recently been demonstrated in mock communities  
499 (Castaño et al., 2020), in our dataset from a natural community PacBio did not recover any

500 reads from the short amplicon library which were longer than those recovered by Illumina and  
501 Ion Torrent. Notably, neither long nor short amplicon sequencing recovered any sequences  
502 identifiable to *Cantharellus*, an ECM genus which is commonly observed at the study sites  
503 as fruitbodies (personal observations by BF and NSY), but which is also known to have  
504 accelerated evolution in the rDNA (Moncalvo et al., 2006) and longer ITS regions than other  
505 fungi (Feibelman et al., 1994), making it an especially difficult target for metabarcoding.  
506 Contrary to expectations, Illumina showed a slightly *higher* fraction of longer ITS2 sequences  
507 than Ion Torrent, which in turn showed slightly longer sequences than PacBio (Figures S7  
508 and S9).

509 The long amplicon dataset included 20% unique taxa, even after clustering at 97% ITS2  
510 similarity, indicating that the differences in the communities recovered are not due to small  
511 sequencing errors, but rather that the different primers capture different parts of the com-  
512 munity. The ITS4 primer used in the short amplicon dataset has known mismatches to  
513 Tulasnellaceae and Alveolata, while gITS7 also has mismatches for Tulasnellaceae (Tedersoo  
514 et al., 2015). ITS1 and LR5 match a much broader range of fungal and other eukaryote  
515 groups (Tedersoo et al., 2015). The alternate LR5-F primer (Tedersoo et al., 2008) would  
516 select against the non-target Alveolata, at the expense of also having mismatches for the  
517 Tulasnellaceae. We assert that, for studies targeting ECM fungi in particular, more com-  
518 plete capture of groups with high rDNA variability such as *Tulasnella* (and ideally other  
519 Cantharellales) is worth the read-depth spent on non-target groups.

### 520 **4.3 Taxonomic identification**

521 Assignment of ecological function to environmental fungal sequences is dependent on accu-  
522 rate taxonomic identification, especially at the genus level or below (Nguyen et al., 2016).  
523 However, different combinations of algorithms and reference datasets vary in their perfor-

524 mance at confidently assigning taxonomy to sequences. Although the RDP fungal training  
525 set and Unite performed comparably at taxonomic placement of long amplicon sequences,  
526 the Warcup database placed notably fewer sequences at all taxonomic levels for all datasets  
527 (Figure 5). This is probably due to two factors. First, the Warcup database does not include  
528 any non-fungi, so it cannot place any non-fungal sequences. Second, due to its low-density  
529 coverage of the fungal kingdom (18 000 sequences vs. 800 000 for Unite), it is likely that  
530 many ITS sequences, especially from uncultured tropical soil fungi, have no close match in  
531 the Warcup database, and so cannot be placed. The RDP fungal training set, which has even  
532 fewer sequences (8000 fungi plus 3000 other eukaryotes), is probably more successful due to  
533 higher sequence conservation in LSU. Heeger et al. (2019) also found that a more conserved  
534 region, in their case 5.8S, outperformed ITS at placing sequences without close database  
535 matches. Of the three algorithms tested, IDTAXA placed fewer sequences than RDPC or  
536 SINTAX with all databases, as expected given its more well-calibrated and conservative con-  
537 fidence scores (Murali et al., 2018), but this was particularly dramatic when paired with the  
538 Warcup database, where IDTAXA placed <25% of ASVs even to phylum.

539 Gdanetz et al. (2017) showed that a majority-rule consensus of three assignment algorithms  
540 can improve the fraction of sequences assigned as well as decrease the false assignment rate.  
541 Strict consensus rejects assignments whenever there is conflict between methods and should  
542 therefore provide more conservative taxonomic assignments than majority-rule consensus.  
543 AMPtk (Palmer et al., 2018) uses a strict consensus taxonomy between UTAX and SINTAX  
544 as an alternative when an initial BLAST search failed to give a hit with at least 97% sequence  
545 identity, but did not present results assessing the results of this approach. Here, we found that  
546 strict consensus also usually increases the number of assigned sequences relative to any single  
547 method, except at family and genus level identifications (Figure 5). Inconsistent family and  
548 genus level assignments are particularly problematic because accurate assignment at these  
549 ranks is generally required for ecological guild assignment using FUNGuild.

550 For ASVs where a long amplicon sequence is available, our novel PHYLOTAX algorithm  
551 uses phylogenetic relationships to resolve these disagreements in a principled manner. The  
552 effect was most pronounced for the PacBio long amplicon dataset, where 46% and 62% of  
553 reads were assigned to genus and family, respectively, by the strict consensus of methods, but  
554 PHYLOTAX increased this fraction to 73% and 81%. This led to a corresponding increase  
555 in the fraction of reads assigned to a functional guild (Figure S16). For short amplicon  
556 sequencing strategies, the improvement was more modest, because PHYLOTAX could only  
557 be applied for ITS2 ASVs with a match to one of the long amplicon ASVs (last row of  
558 Table S2). Deeper long-amplicon sequencing would improve the coverage of long amplicons,  
559 allowing a greater fraction of short amplicon ASVs to also be placed phylogenetically.

#### 560 **4.4 Turnover rate**

561 Mantel correlograms based on the Bray-Curtis dissimilarity (Figure S19) revealed spatial  
562 autocorrelation in the soil fungal community at distance classes  $\leq 3$  m for both Illumina and  
563 PacBio using long and short amplicons, and in the ECM fungal community at distance classes  
564  $\leq 2$  m for Illumina and PacBio long amplicons, and  $\leq 1$  m for the PacBio short amplicons.  
565 These results are similar to autocorrelation ranges found in previous work based on ECM  
566 root tips in temperate forests (Lilleskov et al., 2004; Pickles et al., 2012). Lilleskov et al.  
567 (2004) found autocorrelation only at ranges  $< 2.6$  m at most sites using Sanger sequencing.  
568 Similarly, Pickles et al. (2012) found autocorrelation at distances  $< 3.4$  m based on T-RFLP  
569 analysis. Previous work in Miombo woodland, a similar ecosystem to the Sudanian woodland  
570 in this study, found autocorrelation at ranges  $< 10$  m using Sanger sequencing of ECM root  
571 tips (Tedersoo et al., 2011), which was their smallest distance class.

572 Distance-decay plots (Figure 7, Table S5) gave substantially longer autocorrelation distances.  
573 There was little variation in the results between the Illumina and long-amplicon PacBio

574 datasets for both the total fungal community and the ECM community, with best fit esti-  
575 mates ranging from 12–18 m. The 95% confidence interval was substantially wider than this  
576 variation, generally covering a range of 5–41 m. All of these values are smaller than the 65 m  
577 reported by Bahram et al. (2013), also based on distance-decay curves from a similar ECM  
578 woodland habitat in Benin, but based on Sanger sequencing of ECM root tips rather than  
579 HTS metabarcoding of bulk soil. We speculate that this discrepancy is due to an increased  
580 ability to capture spatially variable rare species using HTS.

581 For the short amplicon dataset, PacBio showed a spatial turnover range more than twice  
582 as long as showed by Illumina (Table S5) for both the total fungi and ECM communities,  
583 with wide confidence intervals. It is possible that the weaker fit for this dataset, which also  
584 showed weaker autocorrelation in the Mantel correlogram, is due to low sequencing depth  
585 in the PacBio short amplicon dataset. The long amplicon PacBio dataset, with more than  
586 twice the read depth of the short amplicon PacBio dataset, gave spatial turnover distance  
587 results much closer to those from Illumina. This is consistent with our speculation that the  
588 longer spatial turnover range found by Bahram et al. (2013) is related to sequence sampling  
589 depth.

590 Year-to-year correlation was found for both the total fungal and ECM communities in the  
591 long amplicon dataset (Figure S19). The spatiotemporal distance-decay fit estimated the  
592 temporal turnover range as 3.3 years for the total fungal community and 4.2 years for the  
593 ECM community, but with overlapping confidence intervals. This corresponds to a space-  
594 for-time substitution rate of 5.4 and 3.3 m/year for the total fungal community and ECM  
595 community, respectively. In a recent study, Kivlin and Hawkes (2020) reported a space-for-  
596 time substitution rate of 81 m/year (reported as 6.8 d / 1.5 m) in the soil fungal community  
597 of a nonseasonal tropical forest in Costa Rica. However, comparison is obscured by different  
598 spatial and temporal sampling scales between the two studies. Year-to-year variation in ECM  
599 fungal communities, which we sampled, has been shown to be less than intra-annual variation

600 (Bahram et al., 2015), as sampled by Kivlin and Hawkes (2020). Neither dataset from the  
601 short amplicon library showed significant temporal autocorrelatio.

602 Weighted UniFrac did not reliably detect spatial structure within this relatively ecologically  
603 homogeneous community. Although the Mantel test did show a small but significant positive  
604 autocorrelation in the fungal community at the smallest size category (1 m; Figure S19),  
605 the distance-decay plot in Figure 7 does not show any clear relationship. The functional  
606 fit showed poor convergence, with a 95% confidence interval for spatial range of 0–5470 m,  
607 indicating little evidence of spatial structure. This is probably because the majority of  
608 community turnover in this system, especially among ECM fungi, is between closely related  
609 species or individuals of the same species, while the presence of major clades (e.g., ECM  
610 lineages *sensu* Tedersoo et al. (2010)) are more spatially constant. This is also reflected  
611 in the generally smaller sample-to-sample dissimilarities measured by UniFrac (0.4–0.6) as  
612 compared to Bray-Curtis (0.8–1.0) in Figure 7. UniFrac analysis would be more suited at  
613 larger spatial scales and/or larger ecological gradients.

## 614 4.5 Conclusion

615 The choice of amplicon and sequencing technology did not affect the results of the spa-  
616 tial analysis, provided sufficient sequencing depth. Alpha diversity estimates were strongly  
617 correlated between methods, but somewhat inflated for Ion Torrent relative to the other  
618 technologies. However, the addition of long amplicon reads did allow the construction of a  
619 phylogenetic tree directly from the metabarcoding reads, which allowed refinement of taxo-  
620 nomic assignments using our new tool PHYLOTAX. DADA2 ASV yield was initially poor  
621 for long amplicons, but this was improved by developing a workflow for extraction of subre-  
622 gions, separate denoising, and then reconstruction of full-length unique sequences. Together  
623 these approaches provide a hybrid approach using long-read sequencing to acquire long am-

624 plicon sequences for the local species pool in order to improve taxonomic assignments, and  
625 cost-effective short-read sequencing to provide high sampling depth and sample number.

## 626 **Acknowledgements**

627 This project was funded by the Swedish research council FORMAS grant number 2014-01109.

628 Laboratory work including PCR and library pooling was performed by Dr. Ylva Strid.

629 The authors would like to acknowledge support of the National Genomics Infrastructure  
630 (NGI) / Uppsala Genome Center and UPPMAX for providing assistance in massive parallel  
631 sequencing and computational infrastructure, funded by RFI / VR and and Science for Life  
632 Laboratory, Sweden.

633 Sequencing was also performed by the SNP&SEQ Technology Platform in Uppsala. The  
634 facility is part of the National Genomics Infrastructure (NGI) Sweden and Science for Life  
635 Laboratory. The SNP&SEQ Platform is also supported by the Swedish Research Council  
636 and the Knut and Alice Wallenberg Foundation.

## 637 **References**

- 638 Abarenkov, K., Somervuo, P., Nilsson, R. H., Kirk, P. M., Huotari, T., Abrego, N., &  
639 Ovaskainen, O. (2018). Protax-fungi: A web-based tool for probabilistic taxonomic  
640 placement of fungal internal transcribed spacer sequences. *New Phytologist*, *220*(2),  
641 517–525. <https://doi.org/10.1111/nph.15301>
- 642 Ainsworth, G. C. (2008). *Ainsworth & Bisby's dictionary of the fungi*. Cabi.
- 643 Altschul, S. F., Gish, W., Miller, W., Myers, E. W., & Lipman, D. J. (1990). Basic local  
644 alignment search tool. *Journal of Molecular Biology*, *215*(3), 403–410. [https://doi.org/10.1016/S0022-2836\(05\)80360-2](https://doi.org/10.1016/S0022-2836(05)80360-2)
- 646 Amir, A., McDonald, D., Navas-Molina, J. A., Kopylova, E., Morton, J. T., Xu, Z. Z., Kight-  
647 ley, E. P., Thompson, L. R., Hyde, E. R., Gonzalez, A., & Knight, R. (2017). Deblur  
648 Rapidly Resolves Single-Nucleotide Community Sequence Patterns. *mSystems*, *2*(2),  
649 e00191–16. <https://doi.org/10.1128/mSystems.00191-16>

- 650 Bahram, M., Koljalg, U., Courty, P.-E., Diedhiou, A. G., Kjølner, R., Polme, S., Ryberg, M.,  
651 Veldre, V., & Tedersoo, L. (2013). The distance decay of similarity in communities of  
652 ectomycorrhizal fungi in different ecosystems and scales. *Journal of Ecology*, *101*(5),  
653 1335–1344.
- 654 Bahram, M., Peay, K. G., & Tedersoo, L. (2015). Local-scale biogeography and spatiotem-  
655 poral variability in communities of mycorrhizal fungi. *New Phytologist*, *205*(4), 1454–  
656 1463. <https://doi.org/10.1111/nph.13206>
- 657 Benson, D. A., Cavanaugh, M., Clark, K., Karsch-Mizrachi, I., Lipman, D. J., Ostell, J., &  
658 Sayers, E. W. (2013). GenBank. *Nucleic Acids Research*, *41*(D1), D36–D42. <https://doi.org/10.1093/nar/gks1195>
- 659
- 660 Berger, S. A., Krompass, D., & Stamatakis, A. (2011). Performance, Accuracy, and Web  
661 Server for Evolutionary Placement of Short Sequence Reads under Maximum Likeli-  
662 hood. *Systematic Biology*, *60*(3), 291–302. <https://doi.org/10.1093/sysbio/syr010>
- 663 Botnen, S. S., Davey, M. L., Halvorsen, R., & Kauserud, H. (2018). Sequence clustering  
664 threshold has little effect on the recovery of microbial community structure. *Molecular*  
665 *Ecology Resources*, *18*(5), 1064–1076. <https://doi.org/10.1111/1755-0998.12894>
- 666 Bray, J. R., & Curtis, J. T. (1957). An Ordination of the Upland Forest Communities of  
667 Southern Wisconsin. *Ecological Monographs*, *27*(4), 326–349. <https://doi.org/10.2307/1942268>
- 668
- 669 Brundrett, M. C. (2017). Global Diversity and Importance of Mycorrhizal and Nonmycor-  
670 rhizal Plants. In L. Tedersoo (Ed.), *Biogeography of Mycorrhizal Symbiosis* (pp. 533–  
671 556). Springer International Publishing. [https://doi.org/10.1007/978-3-319-56363-3\\_21](https://doi.org/10.1007/978-3-319-56363-3_21)
- 672
- 673 Buée, M., Reich, M., Murat, C., Morin, E., Nilsson, R. H., Uroz, S., & Martin, F. (2009). 454  
674 Pyrosequencing analyses of forest soils reveal an unexpectedly high fungal diversity.  
675 *New Phytologist*, *184*(2), 449–456. <https://doi.org/10.1111/j.1469-8137.2009.03003.x>
- 676 Callahan, B. J. (2020a). *DADA2 ITS Pipeline Workflow (1.8)*. Retrieved September 18, 2020,  
677 from [https://benjjneb.github.io/dada2/ITS\\_workflow.html](https://benjjneb.github.io/dada2/ITS_workflow.html)
- 678 Callahan, B. J. (2020b). Frequently Asked Questions: Can I use dada2 with my 454 or Ion  
679 Torrent data? Retrieved September 18, 2020, from <https://benjjneb.github.io/dada2/faq.html#can-i-use-dada2-with-my-454-or-ion-torrent-data>
- 680
- 681 Callahan, B. J., McMurdie, P. J., & Holmes, S. P. (2017). Exact sequence variants should  
682 replace operational taxonomic units in marker-gene data analysis. *The ISME Journal*,  
683 *11*(12), 2639–2643. <https://doi.org/10.1038/ismej.2017.119>
- 684 Callahan, B. J., McMurdie, P. J., Rosen, M. J., Han, A. W., Johnson, A. J. A., & Holmes,  
685 S. P. (2016). DADA2: High-resolution sample inference from Illumina amplicon data.  
686 *Nature Methods*, *13*(7), 581–583. <https://doi.org/10.1038/nmeth.3869>
- 687 Callahan, B. J., Wong, J., Heiner, C., Oh, S., Theriot, C. M., Gulati, A. S., McGill, S. K., &  
688 Dougherty, M. K. (2019). High-throughput amplicon sequencing of the full-length 16S  
689 rRNA gene with single-nucleotide resolution. *Nucleic Acids Research*, *47*(18), e103–  
690 e103. <https://doi.org/10.1093/nar/gkz569>
- 691 Castaño, C., Berlin, A., Durling, M. B., Ihrmark, K., Lindahl, B. D., Stenlid, J., Clemmensen,  
692 K. E., & Olson, Å. (2020). Optimized metabarcoding with Pacific biosciences enables

693 semi-quantitative analysis of fungal communities. *New Phytologist*, 228(3). <https://doi.org/10.1111/nph.16731>

694

695 \_eprint: <https://nph.onlinelibrary.wiley.com/doi/pdf/10.1111/nph.16731>

696 Cole, J. R., Wang, Q., Fish, J. A., Chai, B., McGarrell, D. M., Sun, Y., Brown, C. T.,  
697 Porras-Alfaro, A., Kuske, C. R., & Tiedje, J. M. (2014). Ribosomal Database Project:  
698 Data and tools for high throughput rRNA analysis. *Nucleic Acids Research*, 42(D1),  
699 D633–D642. <https://doi.org/10.1093/nar/gkt1244>

700 Deshpande, V., Wang, Q., Greenfield, P., Charleston, M., Porras-Alfaro, A., Kuske, C. R.,  
701 Cole, J. R., Midgley, D. J., & Tran-Dinh, N. (2016). Fungal identification using a  
702 Bayesian classifier and the Warcup training set of internal transcribed spacer se-  
703 quences. *Mycologia*, 108(1), 1–5. <https://doi.org/10.3852/14-293>

704 Edgar, R. C. (2016a). SINTAX: A simple non-Bayesian taxonomy classifier for 16S and ITS  
705 sequences. *bioRxiv*, 074161. <https://doi.org/10.1101/074161>

706 Edgar, R. C. (2016b). UNOISE2: Improved error-correction for Illumina 16S and ITS ampli-  
707 con sequencing. *bioRxiv*, 081257. <https://doi.org/10.1101/081257>

708 Feibelman, T., Bayman, P., & Cibula, W. G. (1994). Length variation in the internal tran-  
709 scribed spacer of ribosomal DNA in chanterelles. *Mycological Research*, 98(6), 614–  
710 618. [https://doi.org/10.1016/s0953-7562\(09\)80407-3](https://doi.org/10.1016/s0953-7562(09)80407-3)

711 Foster, Z. S. L., Sharpton, T. J., & Grünwald, N. J. (2017). Metacoder: An R package  
712 for visualization and manipulation of community taxonomic diversity data. *PLOS*  
713 *Computational Biology*, 13(2), e1005404. <https://doi.org/10.1371/journal.pcbi.1005404>

714

715 Fouquier, J., Rideout, J. R., Bolyen, E., Chase, J., Shiffer, A., McDonald, D., Knight, R.,  
716 Caporaso, J. G., & Kelley, S. T. (2016). Ghost-tree: Creating hybrid-gene phylogenetic  
717 trees for diversity analyses. *Microbiome*, 4(1), 11. <https://doi.org/10.1186/s40168-016-0153-6>

718

719 [Dataset] Furneaux, B., Bahram, M., Rosling, A., Yorou, N. S., & Ryberg, M. (2020). *Data*  
720 *for "Long- and short-read metabarcoding reveal similar spatio-temporal structures in*  
721 *fungal communities"*. Dryad. <https://doi.org/XXXX>

722 Gdanetz, K., Benucci, G. M. N., Vande Pol, N., & Bonito, G. (2017). CONSTAX: A tool for  
723 improved taxonomic resolution of environmental fungal ITS sequences. *BMC Bioin-*  
724 *formatics*, 18(1), 538. <https://doi.org/10.1186/s12859-017-1952-x>

725 Glassman, S. I., & Martiny, J. B. H. (2018). Broadscale Ecological Patterns Are Robust to  
726 Use of Exact Sequence Variants versus Operational Taxonomic Units. *mSphere*, 3(4).  
727 <https://doi.org/10.1128/mSphere.00148-18>

728 Heeger, F., Wurzbacher, C., Bourne, E. C., Mazzoni, C. J., & Monaghan, M. T. (2019).  
729 Combining the 5.8S and ITS2 to improve classification of fungi. *Methods in Ecology*  
730 *and Evolution*, 10(10), 1702–1711. <https://doi.org/10.1111/2041-210X.13266>

731 \_eprint: <https://besjournals.onlinelibrary.wiley.com/doi/pdf/10.1111/2041-210X.13266>

732 Hollmer, M. (2013). *Roche to close 454 Life Sciences as it reduces gene sequencing focus.*  
733 Retrieved September 18, 2020, from <https://www.fiercebiotech.com/medical-devices/roche-to-close-454-life-sciences-as-it-reduces-gene-sequencing-focus>

734

- 735 Holst-Jensen, A., Vaage, M., Schumacher, T., & Johansen, S. (1999). Structural characteris-  
736 tics and possible horizontal transfer of group I introns between closely related plant  
737 pathogenic fungi. *Molecular Biology and Evolution*, *16*(1), 114–126. [https://doi.org/](https://doi.org/10.1093/oxfordjournals.molbev.a026031)  
738 [10.1093/oxfordjournals.molbev.a026031](https://doi.org/10.1093/oxfordjournals.molbev.a026031)
- 739 Horton, T. R., & Bruns, T. D. (2001). The molecular revolution in ectomycorrhizal ecology:  
740 Peeking into the black-box. *Molecular Ecology*, *10*(8), 1855–1871. [https://doi.org/10.](https://doi.org/10.1046/j.0962-1083.2001.01333.x)  
741 [1046/j.0962-1083.2001.01333.x](https://doi.org/10.1046/j.0962-1083.2001.01333.x)
- 742 House, G. L., Ekanayake, S., Ruan, Y., Schütte, U. M. E., Kaonongbua, W., Fox, G., Ye, Y., &  
743 Bever, J. D. (2016). Phylogenetically Structured Differences in rRNA Gene Sequence  
744 Variation among Species of Arbuscular Mycorrhizal Fungi and Their Implications  
745 for Sequence Clustering. *Applied and Environmental Microbiology*, *82*(16), 4921–4930.  
746 <https://doi.org/10.1128/AEM.00816-16>
- 747 Ihrmark, K., Bödeker, I., Cruz-Martinez, K., Friberg, H., Kubartova, A., Schenck, J., Strid,  
748 Y., Stenlid, J., Brandström-Durling, M., Clemmensen, K. E., et al. (2012). New  
749 primers to amplify the fungal ITS2 region—evaluation by 454-sequencing of artificial  
750 and natural communities. *FEMS Microbiology Ecology*, *82*(3), 666–677.
- 751 Karsch-Mizrachi, I., Takagi, T., Cochrane, G., & Collaboration, o. b. o. t. I. N. S. D. (2018).  
752 The international nucleotide sequence database collaboration. *Nucleic Acids Research*,  
753 *46*(D1), D48–D51. <https://doi.org/10.1093/nar/gkx1097>
- 754 Kennedy, P. G., Cline, L. C., & Song, Z. (2018). Probing promise versus performance in  
755 longer read fungal metabarcoding. *New Phytologist*, *217*(3), 973–976.
- 756 Kivlin, S. N., & Hawkes, C. V. (2020). Spatial and temporal turnover of soil microbial com-  
757 munities is not linked to function in a primary tropical forest. *Ecology*, *101*(4), e02985.  
758 <https://doi.org/10.1002/ecy.2985>  
759 [\\_eprint: https://esajournals.onlinelibrary.wiley.com/doi/pdf/10.1002/ecy.2985](https://doi.org/10.1002/ecy.2985)
- 760 Lanzén, A., Jørgensen, S. L., Huson, D. H., Gorfer, M., Grindhaug, S. H., Jonassen, I., Øvreås,  
761 L., & Urich, T. (2012). CREST – Classification Resources for Environmental Sequence  
762 Tags. *PLOS ONE*, *7*(11), e49334. <https://doi.org/10.1371/journal.pone.0049334>
- 763 Legendre, P., & Legendre, L. F. J. (2012, July 21). *Numerical Ecology*. Elsevier.
- 764 Lilleskov, E. A., Bruns, T. D., Horton, T. R., Taylor, D. L., & Grogan, P. (2004). Detection  
765 of forest stand-level spatial structure in ectomycorrhizal fungal communities. *FEMS*  
766 *Microbiology Ecology*, *49*(2), 319–332. <https://doi.org/10.1016/j.femsec.2004.04.004>
- 767 Lindahl, B. D., Nilsson, R. H., Tedersoo, L., Abarenkov, K., Carlsen, T., Kjøller, R., Kõljalg,  
768 U., Pennanen, T., Rosendahl, S., Stenlid, J., et al. (2013). Fungal community analysis  
769 by high-throughput sequencing of amplified markers—a user’s guide. *New Phytologist*,  
770 *199*(1), 288–299.
- 771 Liu, K.-L., Porras-Alfaro, A., Kuske, C. R., Eichorst, S. A., & Xie, G. (2012). Accurate,  
772 Rapid Taxonomic Classification of Fungal Large-Subunit rRNA Genes. *Applied and*  
773 *Environmental Microbiology*, *78*(5), 1523–1533. [https://doi.org/10.1128/AEM.06826-](https://doi.org/10.1128/AEM.06826-11)  
774 [11](https://doi.org/10.1128/AEM.06826-11)
- 775 Loit, K., Adamson, K., Bahram, M., Puusepp, R., Anslan, S., Kiiker, R., Drenkhan, R., &  
776 Tedersoo, L. (2019). Relative Performance of MinION (Oxford Nanopore Technolo-  
777 gies) versus Sequel (Pacific Biosciences) Third-Generation Sequencing Instruments in

- 778 Identification of Agricultural and Forest Fungal Pathogens. *Applied and Environmental*  
779 *Microbiology*, 85(21). <https://doi.org/10.1128/AEM.01368-19>
- 780 Lozupone, C., & Knight, R. (2005). UniFrac: A New Phylogenetic Method for Comparing  
781 Microbial Communities. *Applied and Environmental Microbiology*, 71(12), 8228–8235.  
782 <https://doi.org/10.1128/AEM.71.12.8228-8235.2005>
- 783 Lozupone, C. A., Hamady, M., Kelley, S. T., & Knight, R. (2007). Quantitative and qual-  
784 itative beta diversity measures lead to different insights into factors that structure  
785 microbial communities. *Applied and Environmental Microbiology*, 73(5), 1576–1585.  
786 <https://doi.org/10.1128/AEM.01996-06>
- 787 Martin, M. (2011). Cutadapt removes adapter sequences from high-throughput sequencing  
788 reads. *EMBnet.journal*, 17(1), 10–12. <https://doi.org/10.14806/ej.17.1.200>
- 789 Matsen, F. A., Kodner, R. B., & Armbrust, E. V. (2010). Pplacer: Linear time maximum-  
790 likelihood and Bayesian phylogenetic placement of sequences onto a fixed reference  
791 tree. *BMC Bioinformatics*, 11(1), 538. <https://doi.org/10.1186/1471-2105-11-538>
- 792 Michot, B., Hassouna, N., & Bachellerie, J.-P. (1984). Secondary structure of mouse 28S  
793 rRNA and general model for the folding of the large rRNA in eukaryotes. *Nucleic*  
794 *Acids Research*, 12(10), 4259–4279. <https://doi.org/10.1093/nar/12.10.4259>
- 795 Moncalvo, J.-M., Nilsson, R. H., Koster, B., Dunham, S. M., Bernauer, T., Matheny, P. B.,  
796 Porter, T. M., Margaritescu, S., Weiß, M., Garnica, S., Danell, E., Langer, G., Langer,  
797 E., Larsson, E., Larsson, K.-H., & Vilgalys, R. (2006). The cantharelloid clade: Deal-  
798 ing with incongruent gene trees and phylogenetic reconstruction methods. *Mycologia*,  
799 *98*(6), 937–948. <https://doi.org/10.1080/15572536.2006.11832623>
- 800 Murali, A., Bhargava, A., & Wright, E. S. (2018). IDTAXA: A novel approach for accurate  
801 taxonomic classification of microbiome sequences. *Microbiome*, 6(1), 140. <https://doi.org/10.1186/s40168-018-0521-5>
- 802
- 803 Nguyen, N. H., Song, Z., Bates, S. T., Branco, S., Tedersoo, L., Menke, J., Schilling, J. S.,  
804 & Kennedy, P. G. (2016). FUNGuild: An open annotation tool for parsing fungal  
805 community datasets by ecological guild. *Fungal Ecology*, 20, 241–248.
- 806 Nilsson, R. H., Ryberg, M., Kristiansson, E., Abarenkov, K., Larsson, K.-H., & Kõljalg, U.  
807 (2006). Taxonomic Reliability of DNA Sequences in Public Sequence Databases: A  
808 Fungal Perspective. *PLOS ONE*, 1(1), e59. [https://doi.org/10.1371/journal.pone.](https://doi.org/10.1371/journal.pone.0000059)  
809 [0000059](https://doi.org/10.1371/journal.pone.0000059)
- 810 Nilsson, R. H., Tedersoo, L., Abarenkov, K., Ryberg, M., Kristiansson, E., Hartmann, M.,  
811 Schoch, C. L., Nylander, J. A. A., Bergsten, J., Porter, T. M., Jumpponen, A.,  
812 Vaishampayan, P., Ovaskainen, O., Hallenberg, N., Bengtsson-Palme, J., Eriksson,  
813 K. M., Larsson, K.-H., Larsson, E., & Kõljalg, U. (2012). Five simple guidelines for  
814 establishing basic authenticity and reliability of newly generated fungal ITS sequences.  
815 *MycoKeys*, 4, 37–63. <https://doi.org/10.3897/mycokeys.4.3606>
- 816 Nilsson, R. H., Wurzbacher, C., Bahram, M., Coimbra, V. R., Larsson, E., Tedersoo, L.,  
817 Eriksson, J., Duarte, C., Svantesson, S., Sánchez-García, M., et al. (2016). Top 50  
818 most wanted fungi. *MycoKeys*, 12, 29.
- 819 Nilsson, R. H., Larsson, K.-H., Taylor, A. F. S., Bengtsson-Palme, J., Jeppesen, T. S., Schigel,  
820 D., Kennedy, P., Picard, K., Glöckner, F. O., Tedersoo, L., Saar, I., Kõljalg, U., &

- 821 Abarenkov, K. (2019). The UNITE database for molecular identification of fungi:  
822 Handling dark taxa and parallel taxonomic classifications. *Nucleic Acids Research*,  
823 47(D1), D259–D264. <https://doi.org/10.1093/nar/gky1022>
- 824 Olson, D. M., Dinerstein, E., Wikramanayake, E. D., Burgess, N. D., Powell, G. V. N.,  
825 Underwood, E. C., D’amico, J. A., Itoua, I., Strand, H. E., Morrison, J. C., Loucks,  
826 C. J., Allnutt, T. F., Ricketts, T. H., Kura, Y., Lamoreux, J. F., Wettengel, W. W.,  
827 Hedao, P., & Kassem, K. R. (2001). Terrestrial Ecoregions of the World: A New Map of  
828 Life on EarthA new global map of terrestrial ecoregions provides an innovative tool for  
829 conserving biodiversity. *BioScience*, 51(11), 933–938. [https://doi.org/10.1641/0006-](https://doi.org/10.1641/0006-3568(2001)051[0933:TEOTWA]2.0.CO;2)  
830 [3568\(2001\)051\[0933:TEOTWA\]2.0.CO;2](https://doi.org/10.1641/0006-3568(2001)051[0933:TEOTWA]2.0.CO;2)
- 831 Öpik, M., Vanatoa, A., Vanatoa, E., Moora, M., Davison, J., Kalwij, J. M., Reier, Ü., &  
832 Zobel, M. (2010). The online database MaarjAM reveals global and ecosystemic  
833 distribution patterns in arbuscular mycorrhizal fungi (Glomeromycota). *New Phytol-*  
834 *ogist*, 188(1), 223–241. <https://doi.org/10.1111/j.1469-8137.2010.03334.x>  
835 [\\_eprint: https://nph.onlinelibrary.wiley.com/doi/pdf/10.1111/j.1469-8137.2010.03334.x](https://nph.onlinelibrary.wiley.com/doi/pdf/10.1111/j.1469-8137.2010.03334.x)
- 836 Pacific Biosciences. (2019). *Consensus library and applications. Contribute to PacificBio-*  
837 *sciences/unanimity development by creating an account on GitHub*. Retrieved March  
838 11, 2019, from <https://github.com/PacificBiosciences/unanimity>
- 839 Palmer, J. M., Jusino, M. A., Banik, M. T., & Lindner, D. L. (2018). Non-biological synthetic  
840 spike-in controls and the AMPtk software pipeline improve mycobiome data. *PeerJ*,  
841 6, e4925. <https://doi.org/10.7717/peerj.4925>
- 842 Pickles, B. J., Genney, D. R., Anderson, I. C., & Alexander, I. J. (2012). Spatial analysis of  
843 ectomycorrhizal fungi reveals that root tip communities are structured by competitive  
844 interactions. *Molecular Ecology*, 21(20), 5110–5123. [https://doi.org/10.1111/j.1365-](https://doi.org/10.1111/j.1365-294X.2012.05739.x)  
845 [294X.2012.05739.x](https://doi.org/10.1111/j.1365-294X.2012.05739.x)
- 846 Rinaldi, A., Comandini, O., & Kuyper, T. W. (2008). Ectomycorrhizal fungal diversity:  
847 Separating the wheat from the chaff. *Fungal Diversity*, 33, 1–45.
- 848 Rognes, T., Flouri, T., Nichols, B., Quince, C., & Mahé, F. (2016). VSEARCH: A versatile  
849 open source tool for metagenomics. *PeerJ*, 4, e2584. [https://doi.org/10.7717/peerj.](https://doi.org/10.7717/peerj.2584)  
850 [2584](https://doi.org/10.7717/peerj.2584)
- 851 Ryberg, M. (2015). Molecular operational taxonomic units as approximations of species in  
852 the light of evolutionary models and empirical data from Fungi. *Molecular Ecology*,  
853 24(23), 5770–5777. <https://doi.org/10.1111/mec.13444>
- 854 Schloss, P. D., Westcott, S. L., Ryabin, T., Hall, J. R., Hartmann, M., Hollister, E. B.,  
855 Lesniewski, R. A., Oakley, B. B., Parks, D. H., Robinson, C. J., Sahl, J. W., Stres, B.,  
856 Thallinger, G. G., Horn, D. J. V., & Weber, C. F. (2009). Introducing mothur: Open-  
857 Source, Platform-Independent, Community-Supported Software for Describing and  
858 Comparing Microbial Communities. *Applied and Environmental Microbiology*, 75(23),  
859 7537–7541. <https://doi.org/10.1128/AEM.01541-09>
- 860 Schoch, C. L., Seifert, K. A., Huhndorf, S., Robert, V., Spouge, J. L., Levesque, C. A., Chen,  
861 W., & Consortium, F. B. (2012). Nuclear ribosomal internal transcribed spacer (ITS)  
862 region as a universal DNA barcode marker for Fungi. *Proceedings of the National*  
863 *Academy of Sciences*, 109(16), 6241–6246. <https://doi.org/10.1073/pnas.1117018109>

- 864 Smith, S. E., & Read, D. J. (2010). *Mycorrhizal symbiosis*. Academic press.
- 865 Somervuo, P., Koskela, S., Pennanen, J., Henrik Nilsson, R., & Ovaskainen, O. (2016). Unbi-  
866 ased probabilistic taxonomic classification for DNA barcoding. *Bioinformatics*, *32*(19),  
867 2920–2927. <https://doi.org/10.1093/bioinformatics/btw346>
- 868 Stamatakis, A. (2014). RAxML version 8: A tool for phylogenetic analysis and post-analysis  
869 of large phylogenies. *Bioinformatics*, *30*(9), 1312–1313. [https://doi.org/10.1093/](https://doi.org/10.1093/bioinformatics/btu033)  
870 [bioinformatics/btu033](https://doi.org/10.1093/bioinformatics/btu033)
- 871 Steidinger, B. S., Crowther, T. W., Liang, J., Van Nuland, M. E., Werner, G. D. A., Reich,  
872 P. B., Nabuurs, G. J., de-Miguel, S., Zhou, M., Picard, N., Herault, B., Zhao, X.,  
873 Zhang, C., Routh, D., & Peay, K. G. (2019). Climatic controls of decomposition drive  
874 the global biogeography of forest-tree symbioses. *Nature*, *569*(7756), 404–408. <https://doi.org/10.1038/s41586-019-1128-0>
- 875
- 876 Steinegger, M., & Salzberg, S. L. (2020). Terminating contamination: Large-scale search  
877 identifies more than 2,000,000 contaminated entries in GenBank. *Genome Biology*,  
878 *21*(1), 115. <https://doi.org/10.1186/s13059-020-02023-1>
- 879 Tedersoo, L., Anslan, S., Bahram, M., Põlme, S., Riit, T., Liiv, I., Kõljalg, U., Kisand, V.,  
880 Nilsson, H., Hildebrand, F., Bork, P., & Abarenkov, K. (2015). Shotgun metagenomes  
881 and multiple primer pair-barcode combinations of amplicons reveal biases in metabar-  
882 coding analyses of fungi. *MycKeys*, *10*, 1–43. [https://doi.org/10.3897/mycokeys.10.](https://doi.org/10.3897/mycokeys.10.4852)  
883 [4852](https://doi.org/10.3897/mycokeys.10.4852)
- 884 Tedersoo, L., Bahram, M., Jairus, T., Bechem, E., Chinoya, S., Mpumba, R., Leal, M.,  
885 Randrianjohany, E., Razafimandimbison, S., Sadam, A., et al. (2011). Spatial structure  
886 and the effects of host and soil environments on communities of ectomycorrhizal fungi  
887 in wooded savannas and rain forests of Continental Africa and Madagascar. *Molecular*  
888 *Ecology*, *20*(14), 3071–3080. Retrieved March 10, 2016, from [http://onlinelibrary.](http://onlinelibrary.wiley.com/doi/10.1111/j.1365-294X.2011.05145.x/full)  
889 [wiley.com/doi/10.1111/j.1365-294X.2011.05145.x/full](http://onlinelibrary.wiley.com/doi/10.1111/j.1365-294X.2011.05145.x/full)
- 890 Tedersoo, L., Jairus, T., Horton, B. M., Abarenkov, K., Suvi, T., Saar, I., & Kõljalg, U.  
891 (2008). Strong Host Preference of Ectomycorrhizal Fungi in a Tasmanian Wet Scle-  
892 rophyll Forest as Revealed by DNA Barcoding and Taxon-Specific Primers. *The New*  
893 *Phytologist*, *180*(2), 479–490.
- 894 Tedersoo, L., May, T. W., & Smith, M. E. (2010). Ectomycorrhizal lifestyle in fungi: Global  
895 diversity, distribution, and evolution of phylogenetic lineages. *Mycorrhiza*, *20*(4), 217–  
896 263.
- 897 Tedersoo, L., Sánchez-Ramírez, S., Kõljalg, U., Bahram, M., Döring, M., Schigel, D., May,  
898 T., Ryberg, M., & Abarenkov, K. (2018). High-level classification of the Fungi and a  
899 tool for evolutionary ecological analyses. *Fungal Diversity*. [https://doi.org/10.1007/](https://doi.org/10.1007/s13225-018-0401-0)  
900 [s13225-018-0401-0](https://doi.org/10.1007/s13225-018-0401-0)
- 901 Tedersoo, L., Tooming-Klunderud, A., & Anslan, S. (2018). PacBio metabarcoding of Fungi  
902 and other eukaryotes: Errors, biases and perspectives. *New Phytologist*, *217*(3), 1370–  
903 1385.
- 904 Urbina, H., Scofield, D. G., Cafaro, M., & Rosling, A. (2016). DNA-metabarcoding uncovers  
905 the diversity of soil-inhabiting fungi in the tropical island of Puerto Rico. *Mycoscience*,  
906 *57*(3), 217–227. <https://doi.org/10.1016/j.myc.2016.02.001>

- 907 Vilgalys, R., & Hester, M. (1990). Rapid genetic identification and mapping of enzymatically  
908 amplified ribosomal DNA from several *Cryptococcus* species. *Journal of Bacteriology*,  
909 *172*(8), 4238–4246. <https://doi.org/10.1128/jb.172.8.4238-4246.1990>
- 910 Wang, Q., Garrity, G. M., Tiedje, J. M., & Cole, J. R. (2007). Naïve Bayesian Classifier  
911 for Rapid Assignment of rRNA Sequences into the New Bacterial Taxonomy. *Appl.*  
912 *Environ. Microbiol.*, *73*(16), 5261–5267. <https://doi.org/10.1128/AEM.00062-07>
- 913 White, T., Bruns, T., Lee, S., & Taylor, J. (1990). Amplification and direct sequencing of  
914 fungal ribosomal RNA genes for phylogenetics. In M. Innis, D. Gelfand, J. Sninsky, &  
915 T. White (Eds.), *PCR Protocols: A Guide to Methods and Applications* (pp. 315–322).  
916 Academic Press, Inc.
- 917 Wong, R. G., Wu, J. R., & Gloor, G. B. (2016). Expanding the UniFrac Toolbox. *PLOS*  
918 *ONE*, *11*(9), e0161196. <https://doi.org/10.1371/journal.pone.0161196>
- 919 Wright, E. S. (2015). DECIPHER: Harnessing local sequence context to improve protein  
920 multiple sequence alignment. *BMC Bioinformatics*, *16*(1), 322. [https://doi.org/10.](https://doi.org/10.1186/s12859-015-0749-z)  
921 [1186/s12859-015-0749-z](https://doi.org/10.1186/s12859-015-0749-z)
- 922 Yang, X., Chockalingam, S. P., & Aluru, S. (2013). A survey of error-correction methods for  
923 next-generation sequencing. *Briefings in Bioinformatics*, *14*(1), 56–66. [https://doi.](https://doi.org/10.1093/bib/bbs015)  
924 [org/10.1093/bib/bbs015](https://doi.org/10.1093/bib/bbs015)
- 925 Yorou, N. S., Koné, N. A., Guissou, M.-L., Guelly, A. K., Maba, D. L., Ekué, M. R. M.,  
926 & De Kesel, A. (2014). Biodiversity and sustainable use of wild edible fungi in the  
927 Soudanian center of endemism: A plea for valorisation. In A. M. Bâ, K. L. McGuire, &  
928 A. G. Diédhiou (Eds.), *Ectomycorrhizal Symbioses in Tropical and Neotropical Forests*  
929 (pp. 241–269). CRC Press. Retrieved August 11, 2020, from [https://scholar.google.](https://scholar.google.com/scholar?hl=en&as_sdt=0%2C5&q=Biodiversity+and+sustainable+use+of+wild+edible+fungi+in+the+soudanian+center+of+endemism&btnG=)  
930 [com/scholar?hl=en&as\\_sdt=0%2C5&q=Biodiversity+and+sustainable+use+of+](https://scholar?hl=en&as_sdt=0%2C5&q=Biodiversity+and+sustainable+use+of+wild+edible+fungi+in+the+soudanian+center+of+endemism&btnG=)  
931 [wild+edible+fungi+in+the+soudanian+center+of+endemism&btnG=](https://scholar?hl=en&as_sdt=0%2C5&q=Biodiversity+and+sustainable+use+of+wild+edible+fungi+in+the+soudanian+center+of+endemism&btnG=)

## 932 Data Accessibility

- 933 • Trimmed, demultiplexed sequencing reads have been deposited at the European Nu-  
934 cleotide Archive (ERA) under Project accession number PRJEB37385. Accession num-  
935 bers are given in Supplementary Files 1 and 2.
- 936 • Consensus ASV sequences will also be deposited at ENA prior to publication.
- 937 • Nucleotide alignment and ML tree will be deposited at Dryad prior to final publication  
938 (Furneau et al., 2020).
- 939 • R packages `LSUx`, `tzara`, `phylotax`, and `FUNGuildR` are available on Github at

940 <https://github.com/brendanf/LSUx>, <https://github.com/brendanf/tzara>, <https://github.com/brendanf/phyloTax>, and <https://github.com/brendanf/FUNGuildR>.  
941  
942 These packages are currently being prepared for submission to CRAN/Bioconductor.  
943 If they are not accepted prior to final publication, snapshots will be archived at Dryad.  
944 • FASTA-format files for the RDP, Warcup, and Unite reference databases with unified  
945 classifications, as well as scripts used to generate them, are available at <https://github.com/brendanf/reannotate>. The versions used in this paper will be archived at Dryad  
946 prior to publication.  
947  
948 • Bioinformatics pipeline and analysis scripts are available at <https://github.com/oueme-fungi/oueme-fungi-transect>.  
949

## 950 **Author Contributions**

951 Sampling was planned and carried out by BF, NSY, and MR. Bioinformatics and data analysis  
952 were performed by BF with input from MB, AR, and MR. Scripts and R packages were  
953 written by BF. The manuscript was drafted by BF and MR. All authors contributed to and  
954 approved the final version of the manuscript.

955 **List of Figures**

956 1 rDNA regions . . . . . 37  
957 2 Shared richness and abundance of ASVs and OTUs between different sequenc-  
958 ing technologies . . . . . 38  
959 3 ASV accumulation curves . . . . . 39  
960 4 Comparison of ASV richness between sequencing technologies . . . . . 40  
961 5 Summary of taxonomic assignments . . . . . 41  
962 6 Taxonomic composition of fungal community at the class level . . . . . 42  
963 7 Distance-decay plot for community dissimilarities and spatio-temporal distance 43

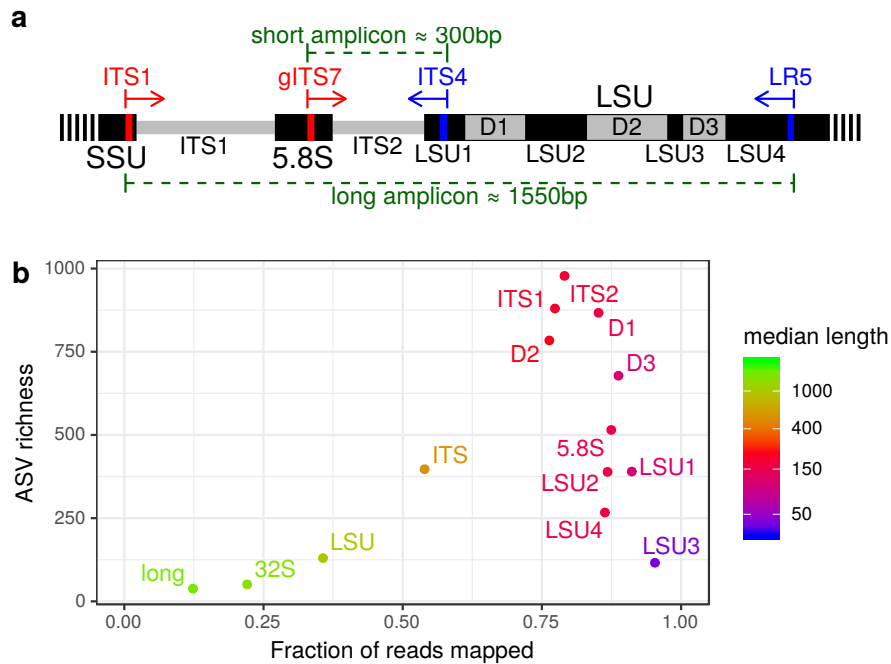


Figure 1: rDNA regions. **(a)** Partial map of rDNA showing the 5.8S rDNA, partial SSU and LSU rDNA, and internally transcribed spacer (ITS) regions. D1–3 represent the first three variable regions in LSU, while LSU1–4 represent the conserved regions. Primer sites used in this study are indicated in red (forward primers) and blue (reverse primers), and the resulting amplicons are shown with green braces. **(b)** Total number of DADA2 ASVs vs. fraction of demultiplexed reads successfully mapped to ASVs for different rDNA regions extracted from a set of long PacBio amplicon sequences using LSU $x$ . Shorter and more conserved regions yield a greater fraction of successfully mapped reads. At a given fraction of mapped reads, more variable regions yield a greater number of unique ASVs.

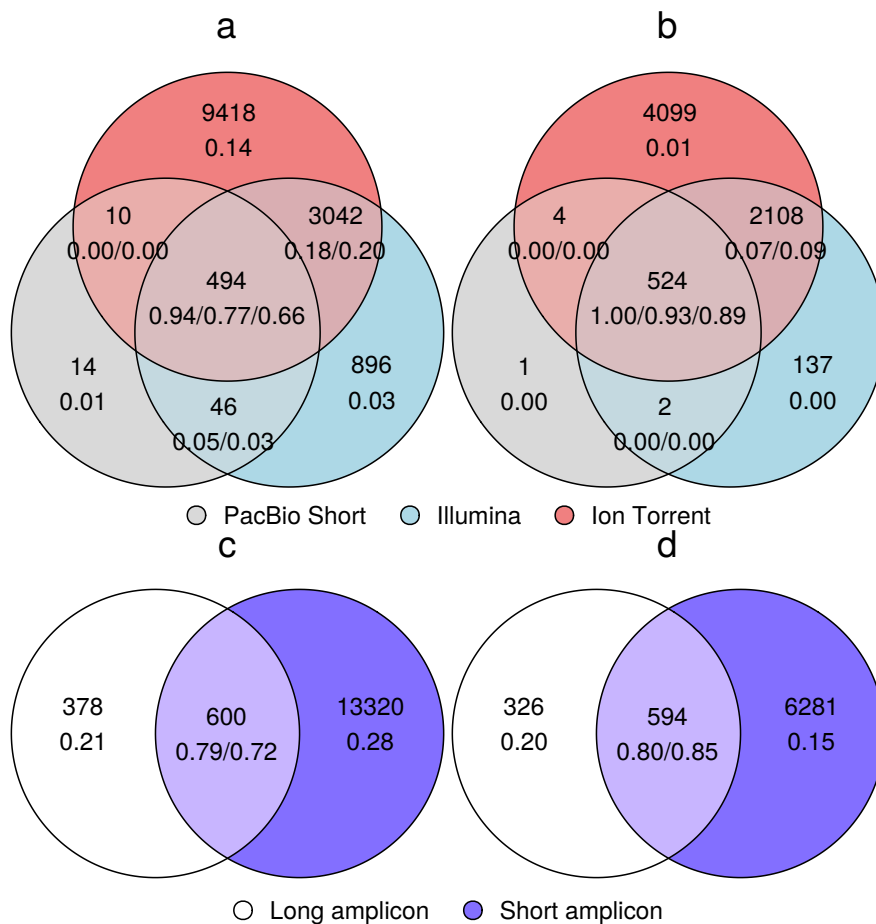


Figure 2: Shared richness and abundance of ITS2-based ASVs (*a*, *c*) and 97% OTUs (*b*, *d*) between different sequencing technologies from the same short amplicon library (*a*, *b*), and between long and short amplicon libraries (*c*, *d*). In each region, the ASV/OTU richness is given above, while the relative abundance of reads represented by these ASVs/OTUs in each sequencing strategy are shown below in the order PacBio/Illumina/Ion Torrent (*a*, *b*), or long/short (*c*, *d*). For short amplicons in *c* and *d*, ASV/OTU counts reflect detection by any of the three technologies, and read counts represent the mean fraction of reads across the three technologies.

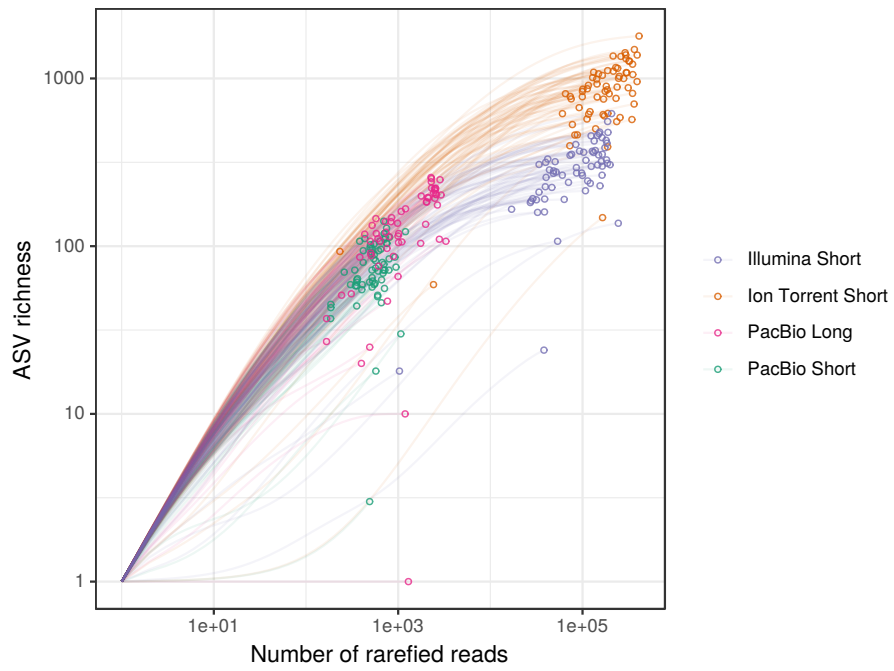


Figure 3: ASV accumulation curves. Each curve represents rarefaction of a single sample or pooled pair of samples. Points at the end of each curve represent the actual read depth and observed ASV richness. Note logarithmic axes.

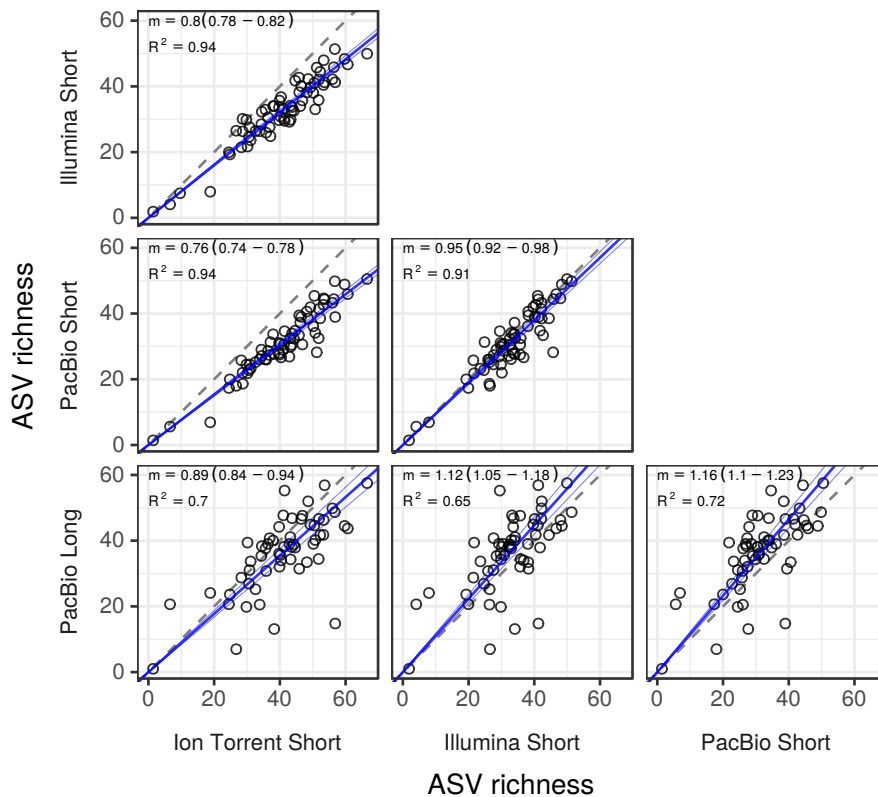


Figure 4: Comparison of ASV richness between sequencing technologies. Each point represents the richness of one or two pooled samples, as determined by two different sequencing strategies. All values represent the average of 100 replicate rarefactions with a sample depth of 100 reads. Because samples in the same well on different plates could not be demultiplexed in the Ion Torrent dataset, these samples were also bioinformatically pooled in the other datasets prior to rarefaction. Blue lines are total least squares fit with 95% confidence interval, with the given slope (and 95% confidence interval) and  $R^2$  value. Dashed diagonal line indicates ideal slope of 1.

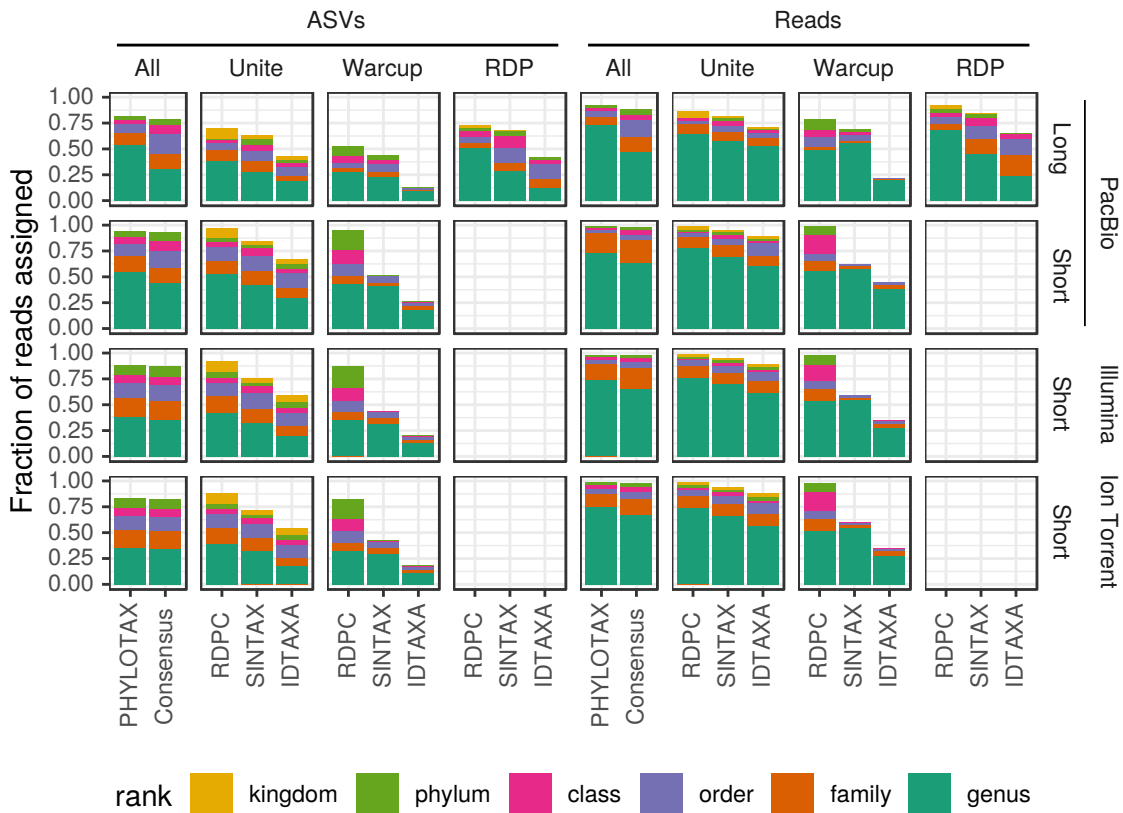


Figure 5: Fraction of ASVs (left) and reads (right) assigned to each taxonomic rank, for different sequencing technologies (PacBio RS II, Illumina MiSeq, Ion Torrent Ion S5), amplicons (Long, Short), reference databases (Unite, Warcup, RDP), and assignment algorithms (PHYLOTAX, Consensus, RDPC, SINTAX, IDTAXA). Consensus and PHYLOTAX assignments are based on the consensus of RDPC, SINTAX, and IDTAXA, using all available databases and, in the case of PHYLOTAX, phylogenetic information.

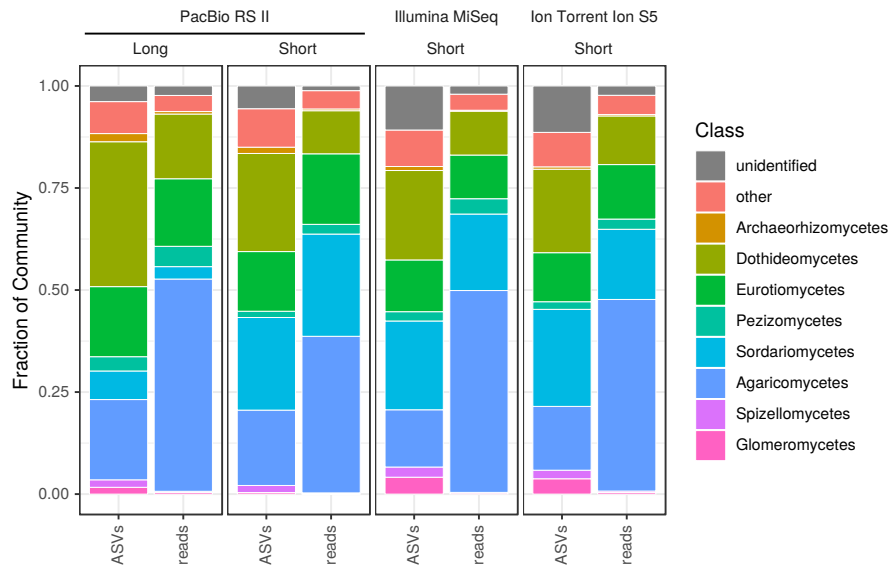


Figure 6: Taxonomic composition of fungal community at the class level. Values represent the fraction of all ASVs and reads which were assigned to kingdom Fungi. Assignments based on PHYLOTAX. Classes which represented less than 2% of reads and ASVs in all datasets are grouped together as “other”.

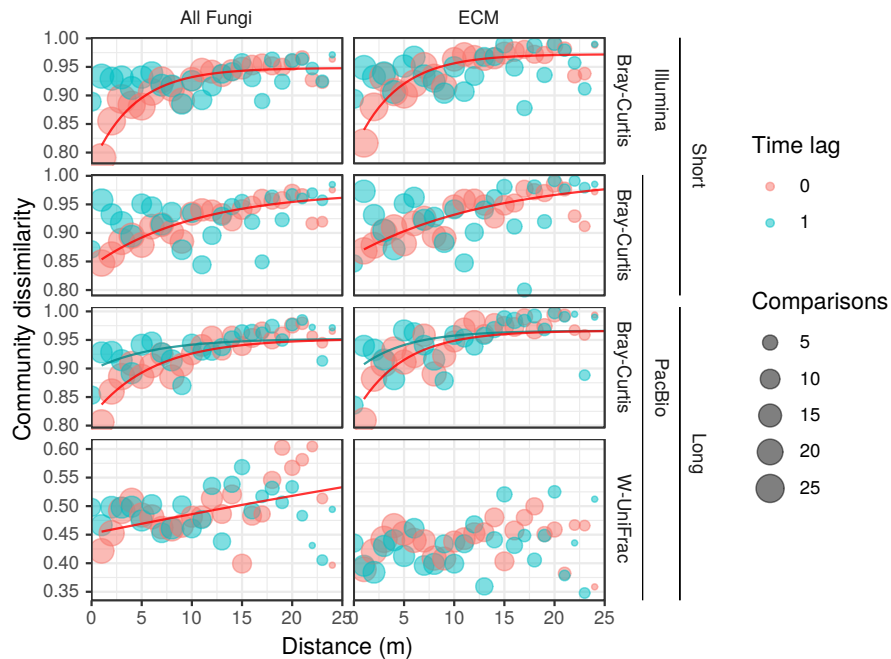


Figure 7: Distance-decay plot for community dissimilarities and spatio-temporal distance. Circles represent community data from short (top two rows) and long (bottom two rows) amplicon libraries, sequenced by Illumina MiSeq (top row) or PacBio RS II (bottom three rows). Community dissimilarities are calculated using the Bray-Curtis dissimilarity for all datasets (top three rows) and using the weighted UniFrac dissimilarity for the long amplicon library, for which a phylogenetic tree could be constructed (bottom row). The left column represents the full fungal community, and the right column only sequences identified as ECM. The color of each circle represents the time lag between samples being compared (0 or 1 year), and the size represents the number of comparisons for that spatial distance and time lag. Lines are the best-fit lines for an exponential decay to max model. The model was only fit for datasets where the Mantel test indicated a significant relationship between community dissimilarity and spatial (for the 0 year time lag) or spatiotemporal (for the 1 year time lag) distance.